On the P-SBAS processing chain new developments for the generation of SAOCOM-1 Advanced DInSAR products

Claudio De Luca, Yenni Lorena Belen Roa, Manuela Bonano, Francesco Casu, Leonardo Euillades, Pablo Euillades, Marianna Franzese, Michele Manunta, Yasir Muhammad, Giovanni Onorato, Pasquale Striano, Ivana Zinno and Riccardo Lanari

(1) Istituto per il Rilevamento Elettromagnetico dell'Ambiente (IREA), CNR, Napoli, Italy
(2) Conicet, Instituto CEDIAC, Facultad de Ingenierìa, Universidad Nac de Cuyo, Mendoza, Argentina

FRINGE 2023
University of Leeds, UK | 11 - 15 September 2023.

MOTIVATION

The effectiveness of the satellite DInSAR technology for ground deformation analyses, and its crucial role in emergency scenarios, are pushing the space agencies to develop new space-borne SAR systems. In particular, important investments on the development of L-band SAR systems are ongoing, with the forthcoming missions of ESA (ROSE-L), JAXA (PALSAR-3) and NASA-ISRO (NISAR), as well as the already operating **SAOCOM-1** and PALSAR-2 systems.

OUTLINE

- **SAOCOM-1** constellation characteristics.
- Development of procedure for the large scale monitoring service implementation.
- Preliminary results of the P-SBAS processing chain with SAOCOM-1 data, which clearly show the relevance of these sensors for what attains their DInSAR applications.
- Open Issues

ACKNOWLEDGEMENT

The activities of this work were carried out within the project referred to as DInSAR-3M, funded by the Italian Space Agency (ASI)

SAOCOM-1 constellation (SAOCOM-1A and -1B)

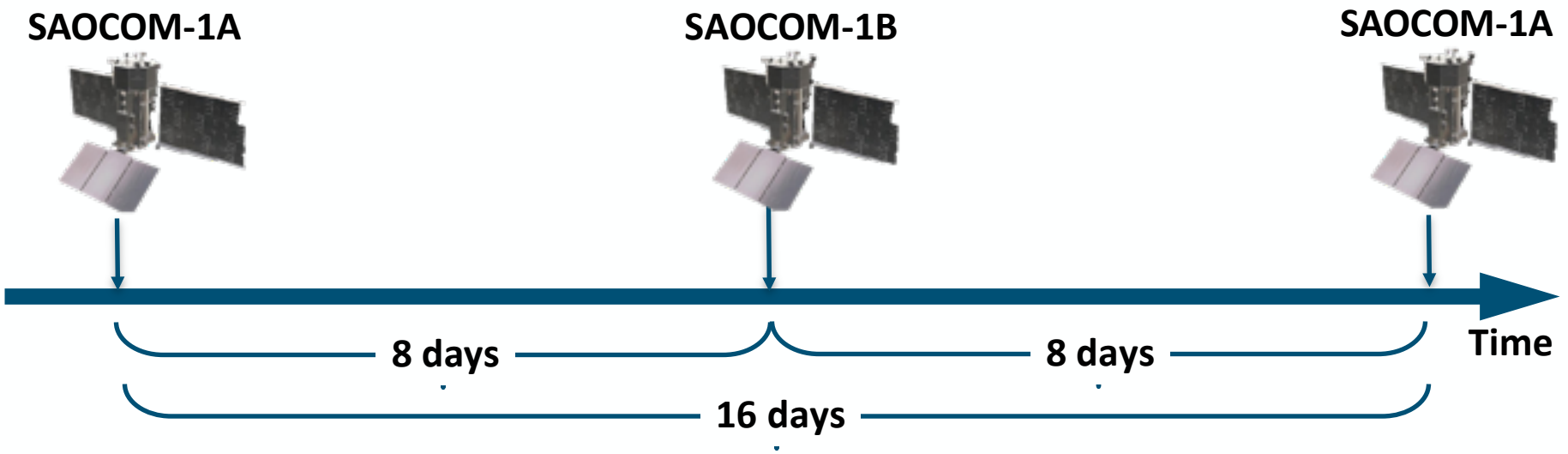

The Argentinian constellation SAOCOM-1A and 1B and the Italian COSMO-SkyMed create the SIASGE system orbiting on the **same paths**.

- Spatial resolution (stripmap mode): **5 m x 5 m** (Single e Dual Pol)
  5 m x 6 m (Quad Pol)

- Footprint: **40-60 km** (Single e Dual Pol) **20-30 km** (Quad Pol)
  Banda L ($\lambda \cong 23.5\ cm$)

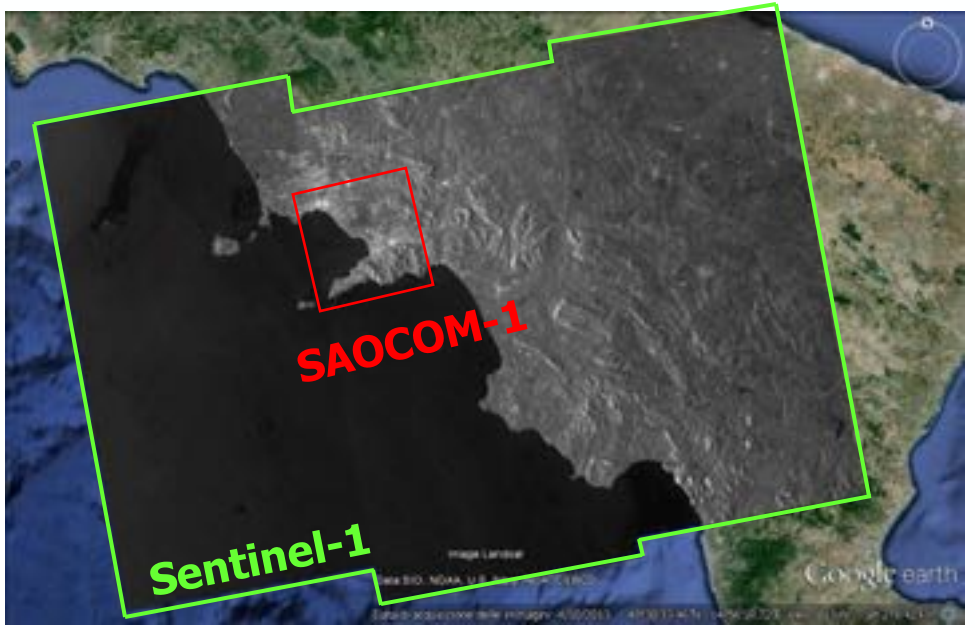

Development of procedures for large scale monitoring service implementation

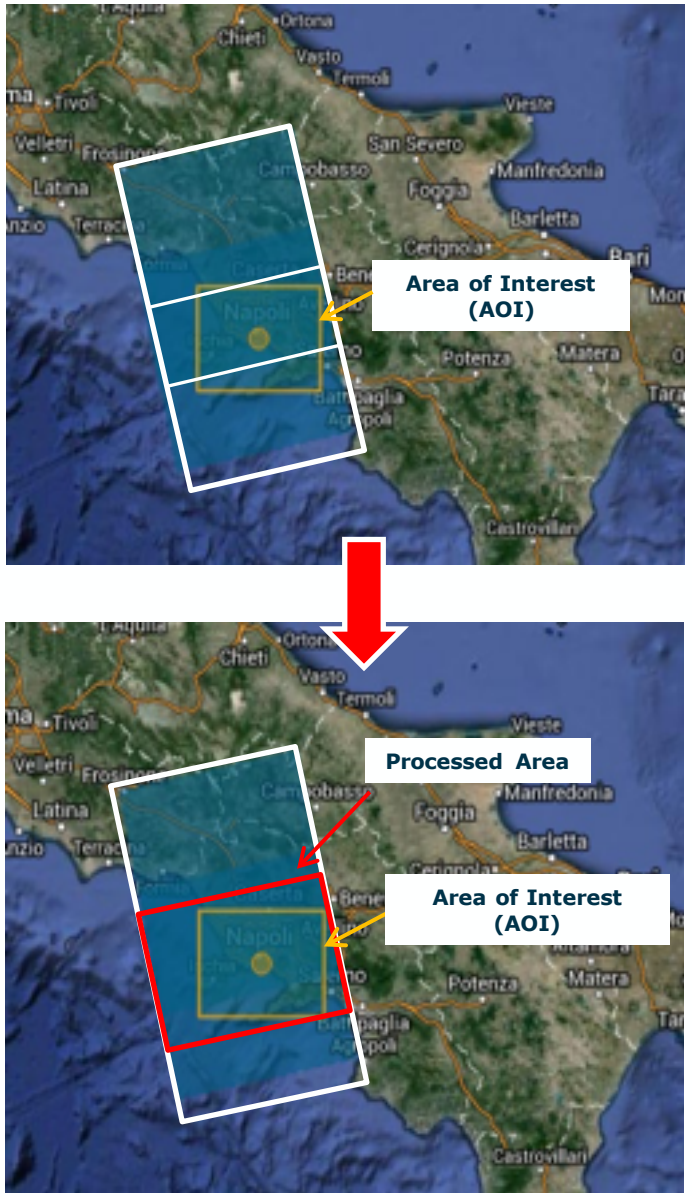

Block diagram of the implemented procedure related to the ingestion, merging and cut of the **SAOCOM L1A SAR data**.

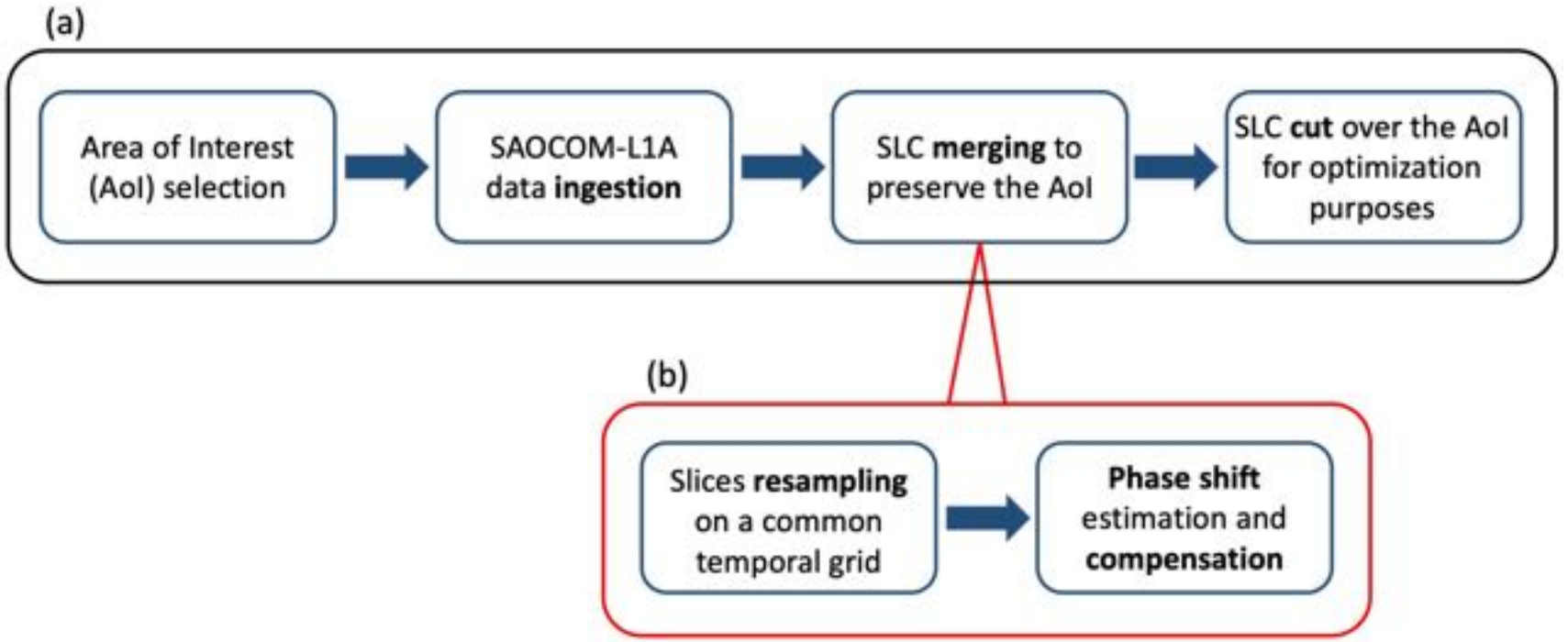

Development of procedures for large scale monitoring service implementation

Slices resampling on a common temporal grid

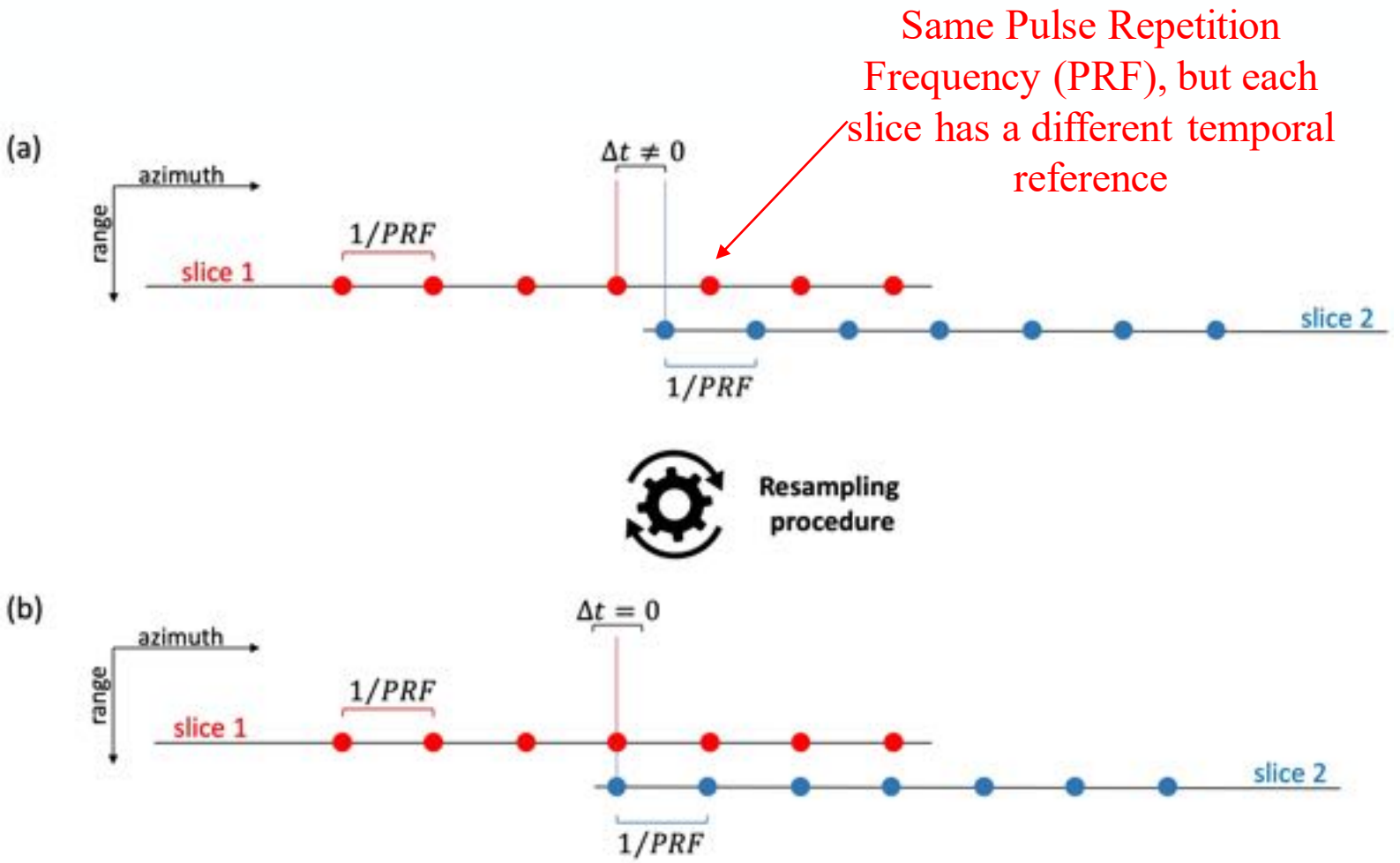

Pictorial scheme of the temporal resampling procedure that has been implemented for the merging procedure.

(a) represents the temporal shift between two adjacent SAOCOM slices.

(b) is the result after the resampling procedure, where the second slice is computed on the temporal grid of the first one.

Development of procedures for large scale monitoring service implementation

Phase shift estimation and compensation procedure

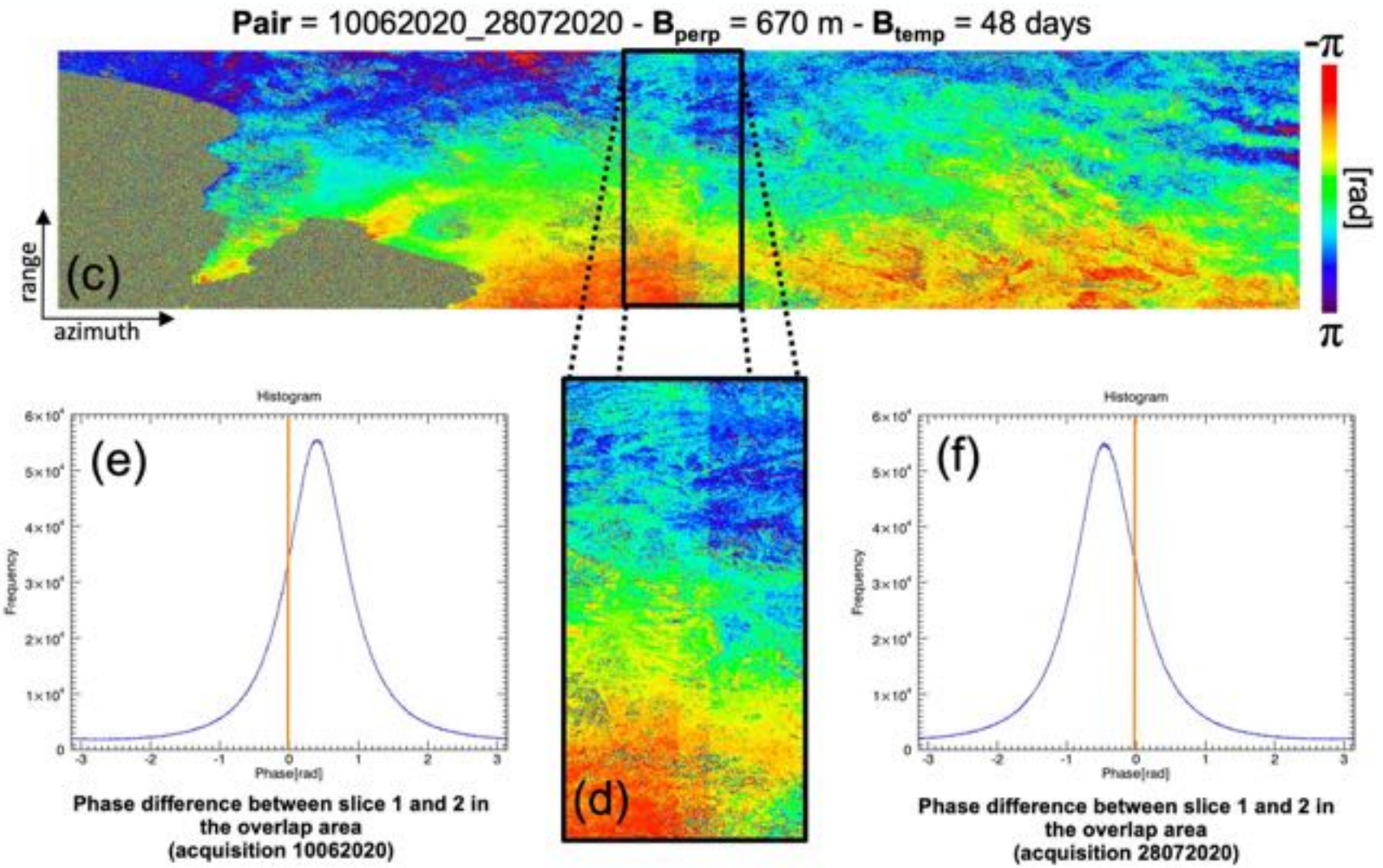

Master Image

Acquisition date: 10062020

Slave Image

Acquisition date: 28072020

Development of procedures for large scale monitoring service implementation

Phase shift estimation and compensation procedure

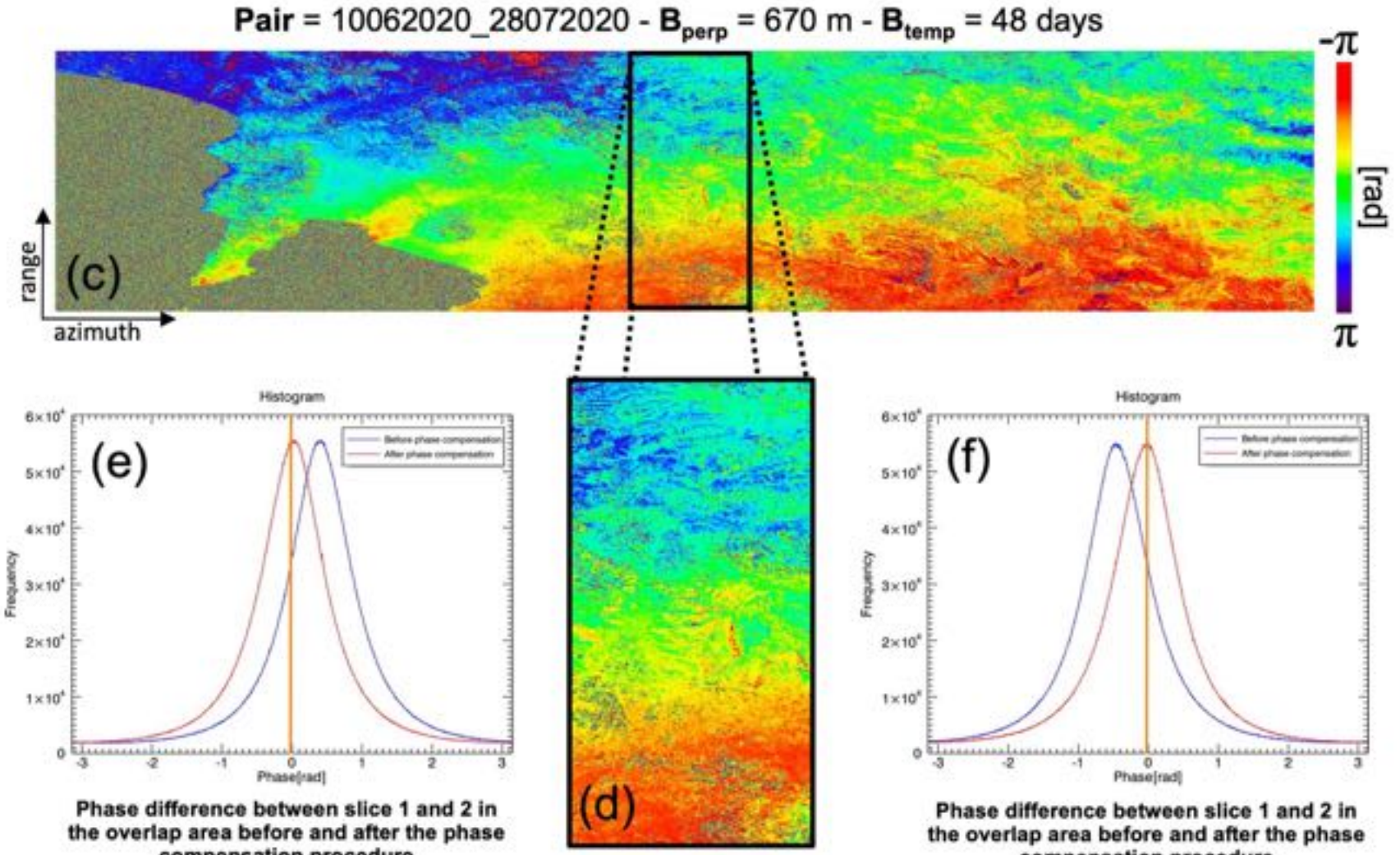

Phase difference between slice 1 and 2 in the overlap area before and after the phase compensation procedure (acquisition 10062020)

Phase difference between slice 1 and 2 in the overlap area before and after the phase compensation procedure (acquisition 28072020)

Master Image

Acquisition date: 10062020

Slave Image

Acquisition date: 28072020

Development of procedures for large scale monitoring service implementation

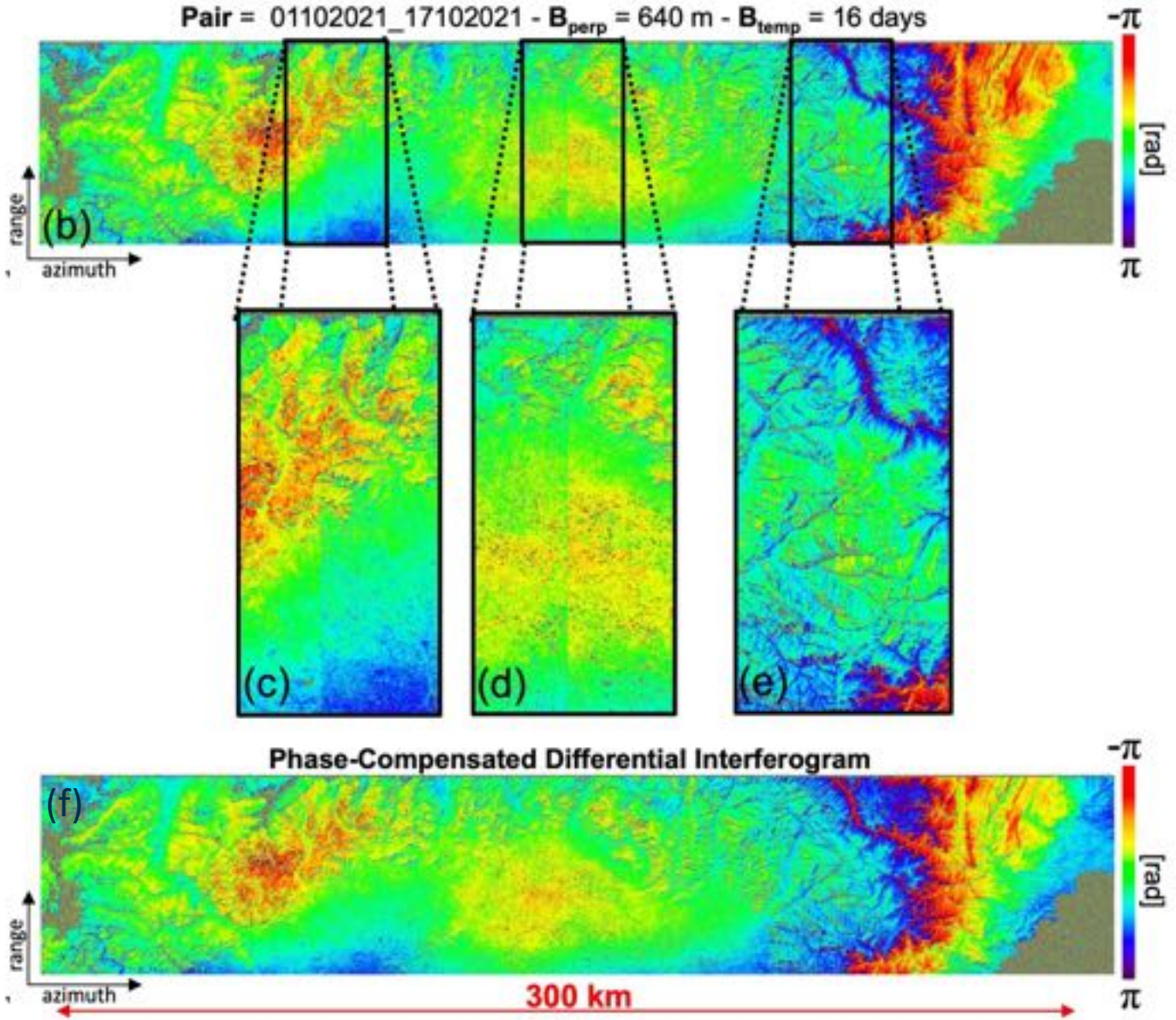

Multiple-slice phase shift estimation and compensation

Development of procedures for large scale monitoring service implementation

Residual orbital ramps estimation and removal

Acquisition date and orbit accuracy	
Ascending path	
Acquisition Date	**Orbit**
02-01-2020	(OLF)
19-02-2020	(OLF)
20-01-2021	(OLVF)
13-06-2021	(OLVF)

OL = OnLine, available 18 days later

OLF = OffLine_Fast, processed after 2 days

OLVF = OnLine_Very_Fast, processed with on board GPS

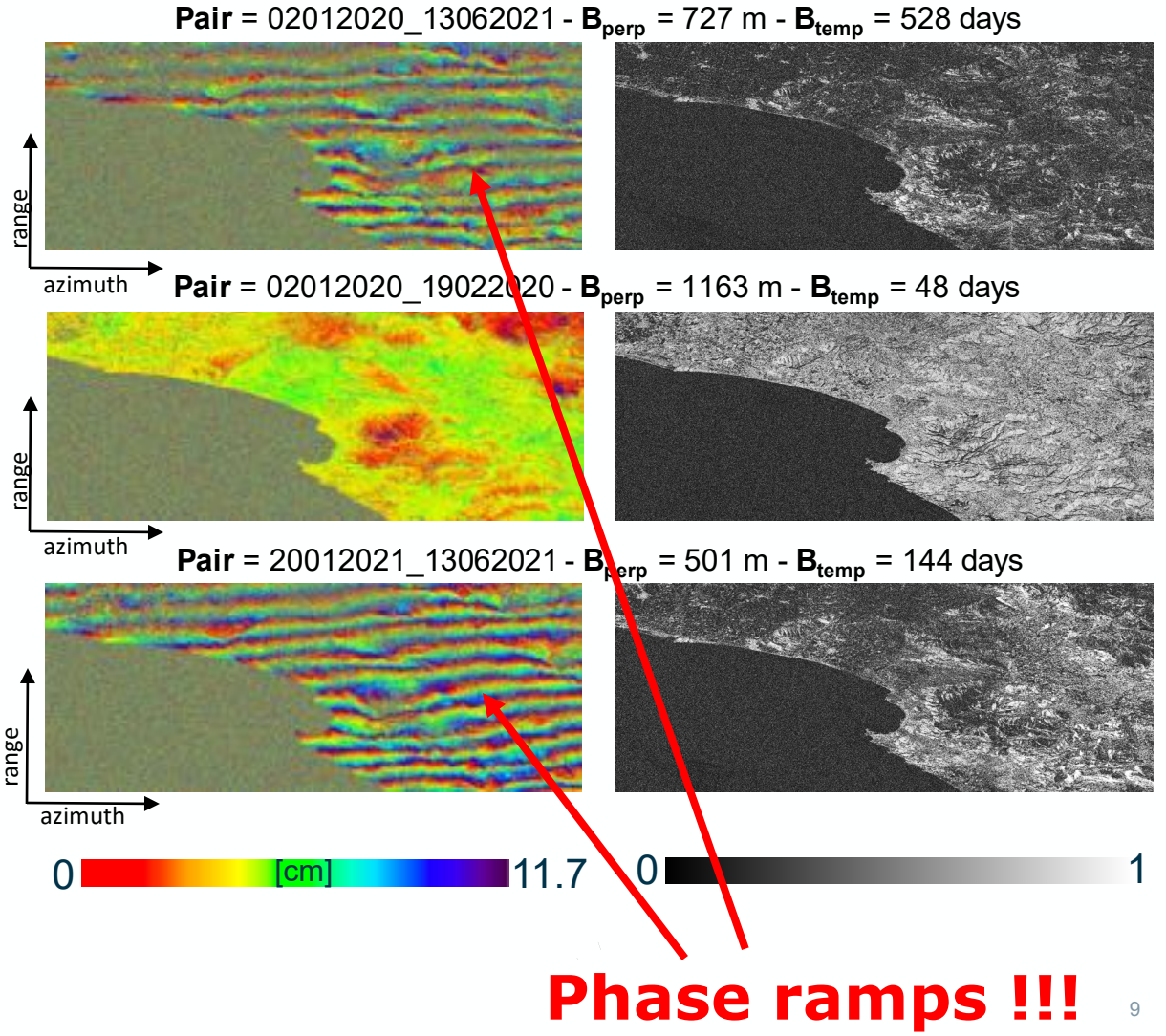

Stripmap P-SBAS processing chain for SAOCOM L1A data processing

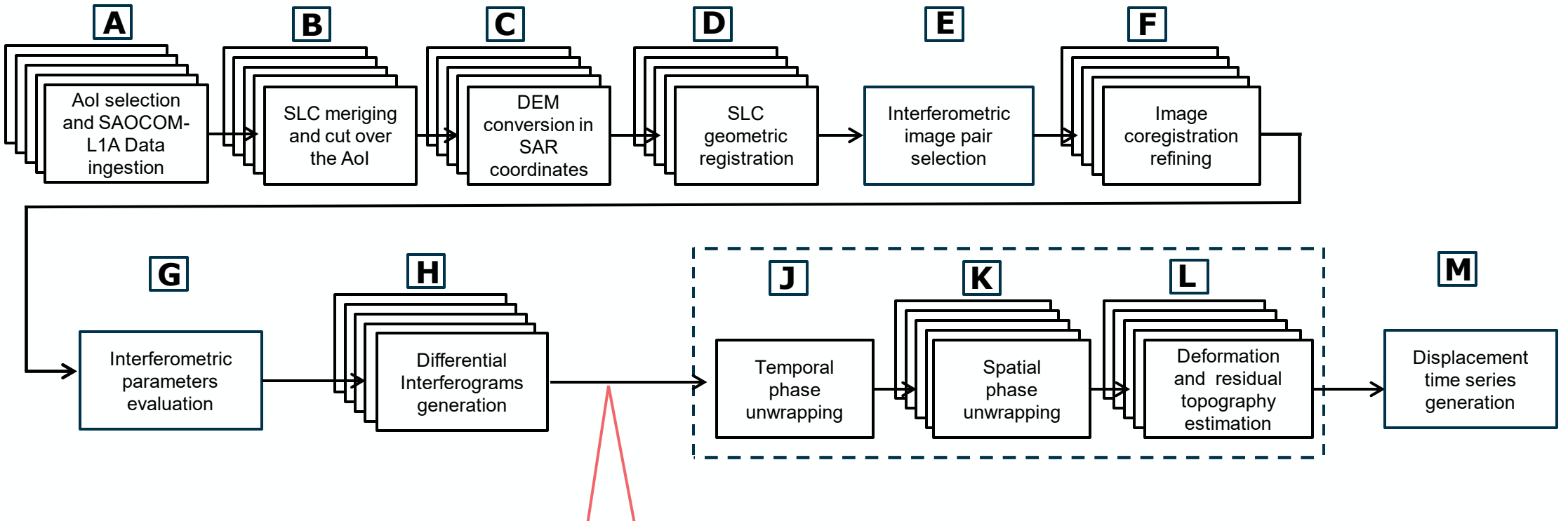

I

residual orbital ramps estimation and removal

- Two–dimensional Discrete Fourier Transformation (2D-DFT)
- Estimation of the orbit correction for each SAR acquisition of our time-series (Pepe, A., Berardino, P., Bonano, M., Euillades, L. D., Lanari, R., & Sansosti, E. (2011)).

Stripmap P-SBAS processing chain for SAOCOM L1A data processing

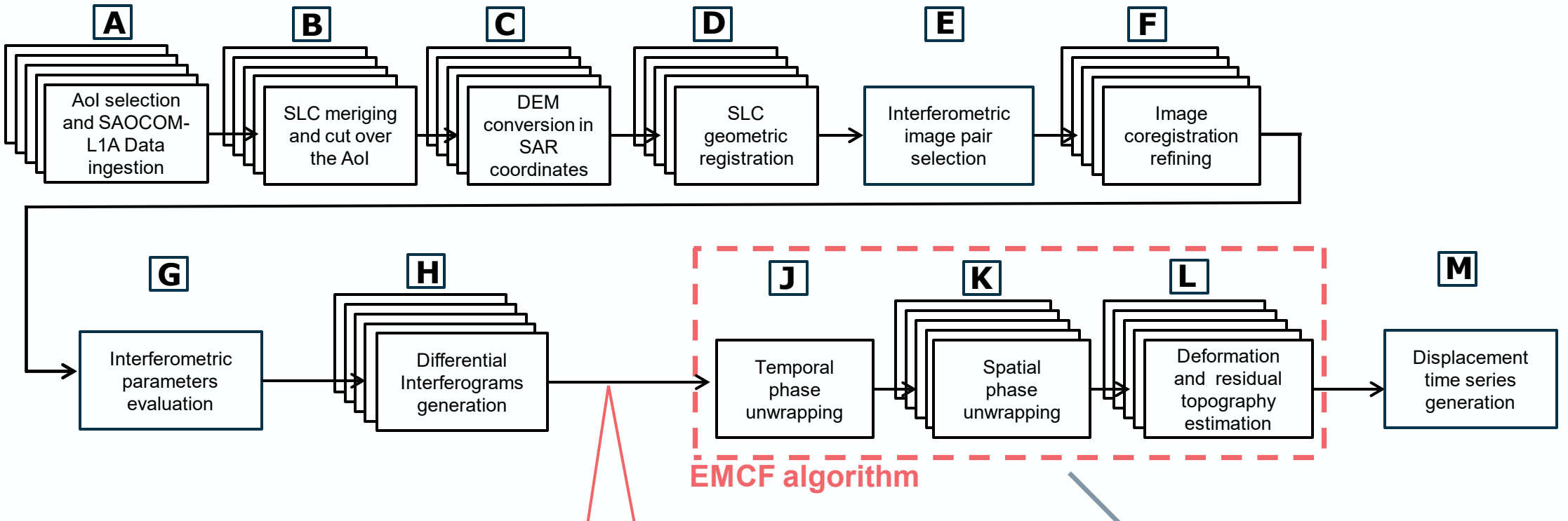

I

residual orbital ramps estimation and removal

- Two–dimensional Discrete Fourier Transformation (2D-DFT)
- Estimation of the orbit correction for each SAR acquisition of our time-series (Pepe, A., Berardino, P., Bonano, M., Euillades, L. D., Lanari, R., & Sansosti, E. (2011)).

New PhU advances can be done compared to the standard Extended Minimum Cost Flow (EMCF) algorithm by benefiting of the **higher number of Small-Baseline interferograms**

Stripmap P-SBAS processing chain for SAOCOM L1A data processing: PhU problem

Napoli Bay Area

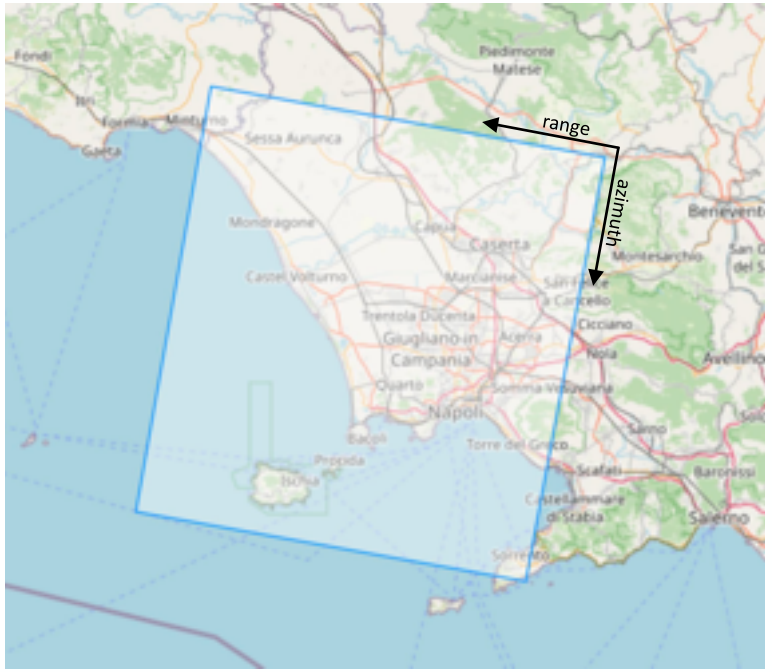

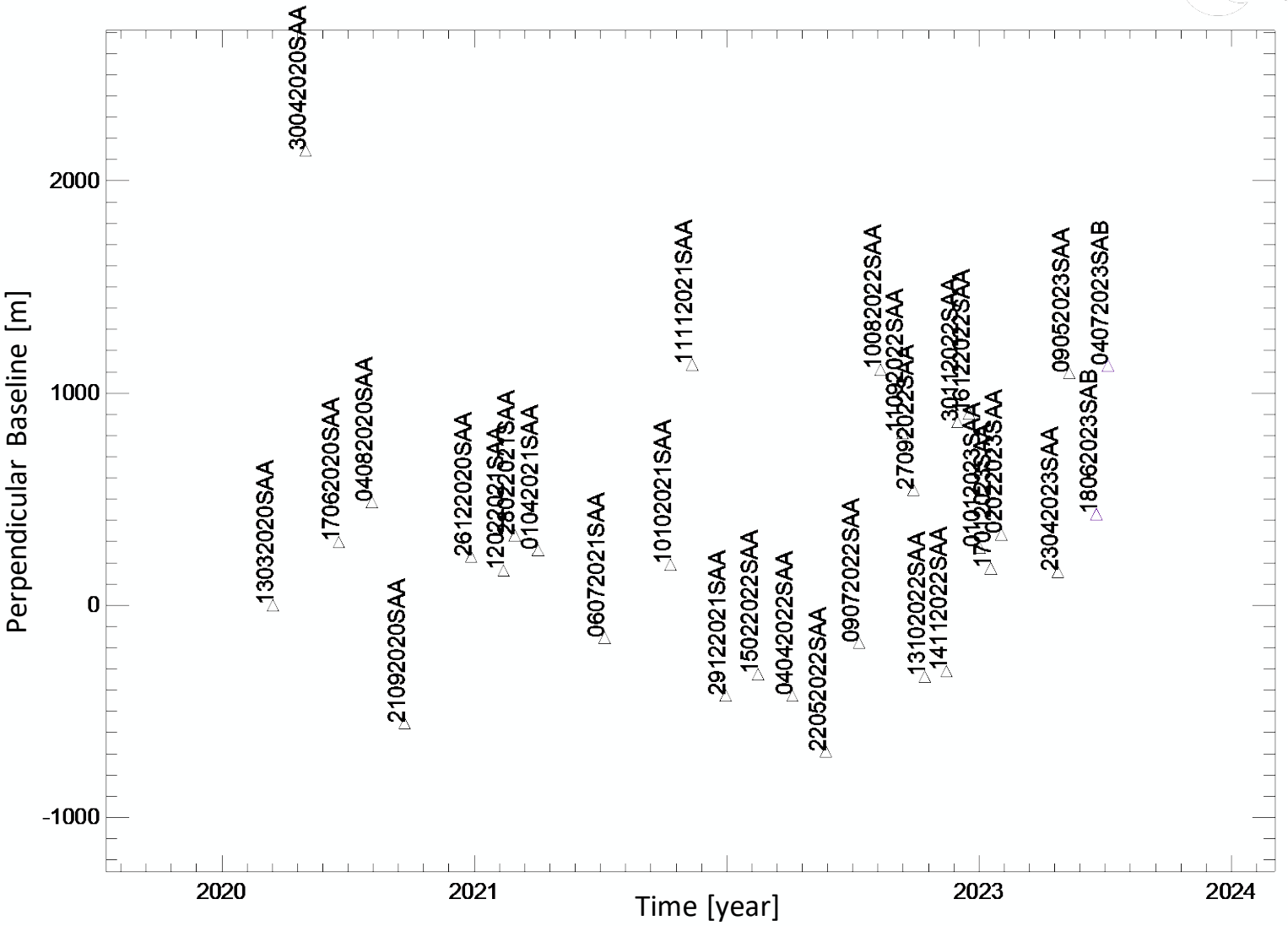

A. Pepe and R. Lanari, "On the Extension of the Minimum Cost Flow Algorithm for Phase Unwrapping of Multitemporal Differential SAR Interferograms," in *IEEE Transactions on Geoscience and Remote Sensing*, vol. 44, no. 9, pp. 2374-2383, Sept. 2006,

Stripmap P-SBAS processing chain for SAOCOM L1A data processing: PhU problem

Napoli Bay Area

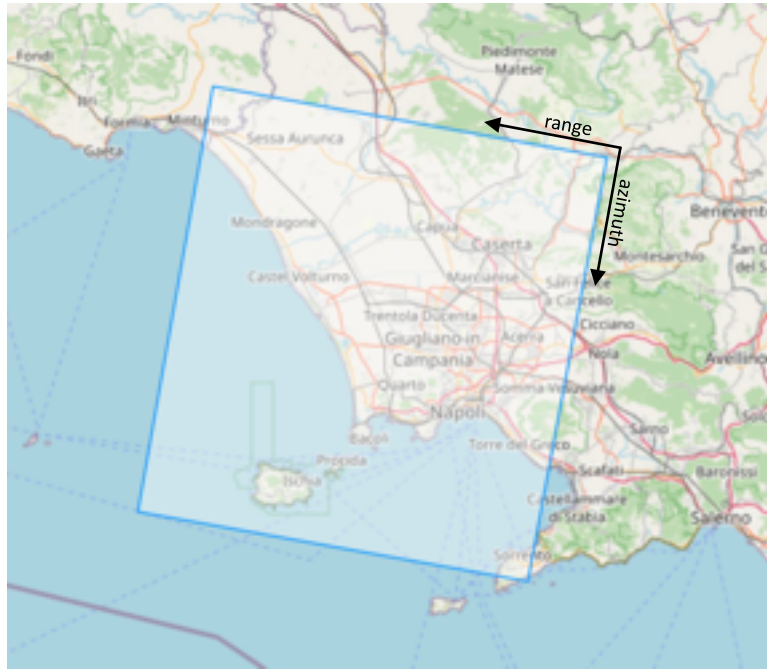

Delaunay Triangolation

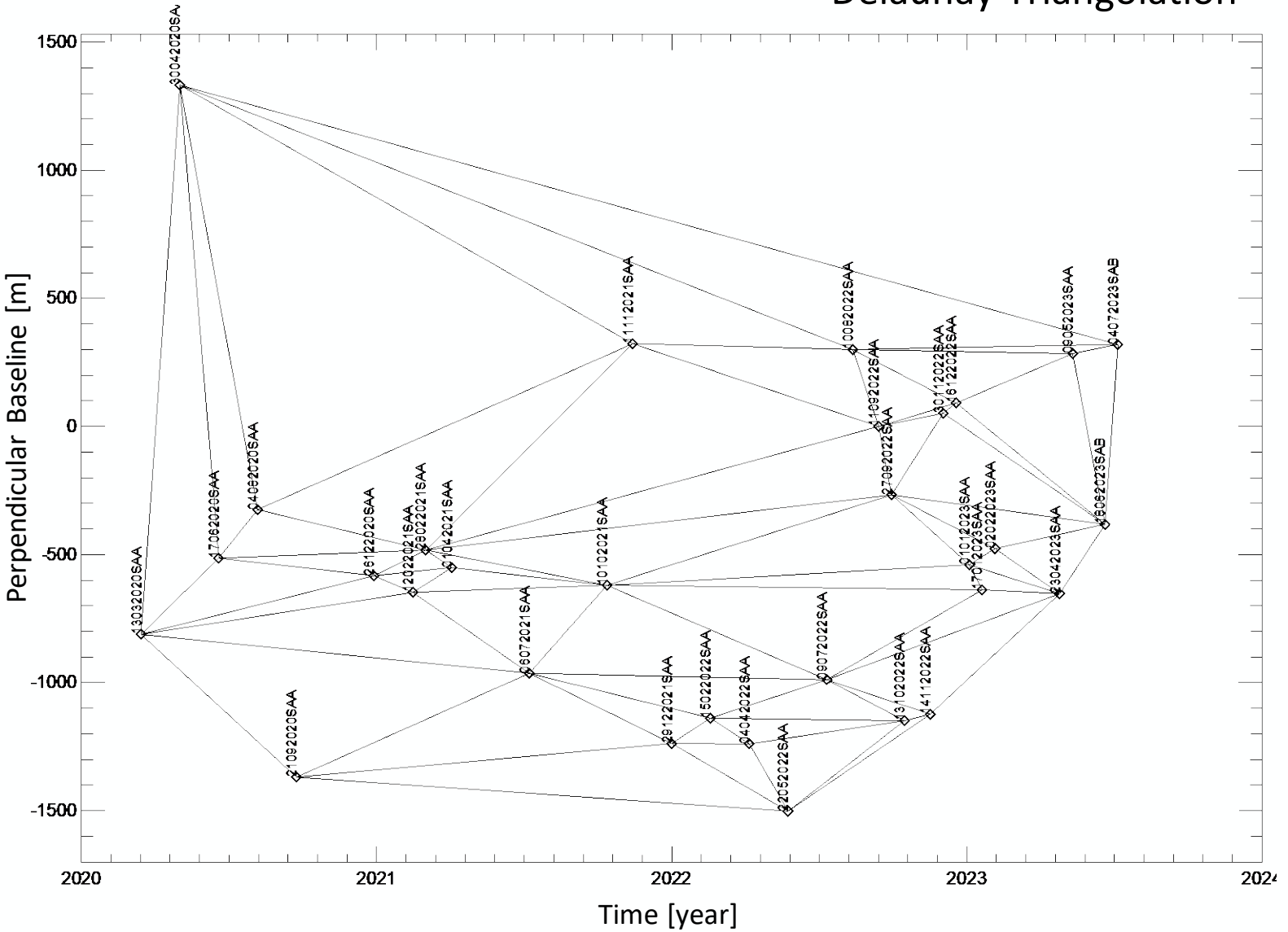

Stripmap P-SBAS processing chain for SAOCOM L1A data processing: PhU problem

Napoli Bay Area

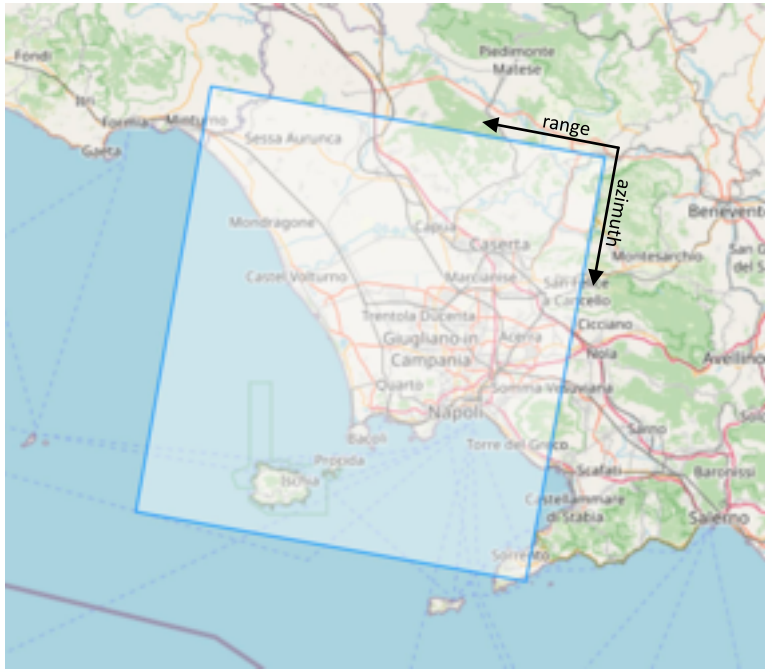

Baseline constraints

Temporal Baseline <= 600 days

Perpendicular Baseline <= 1500 m

Reduced Delaunay Triangolation

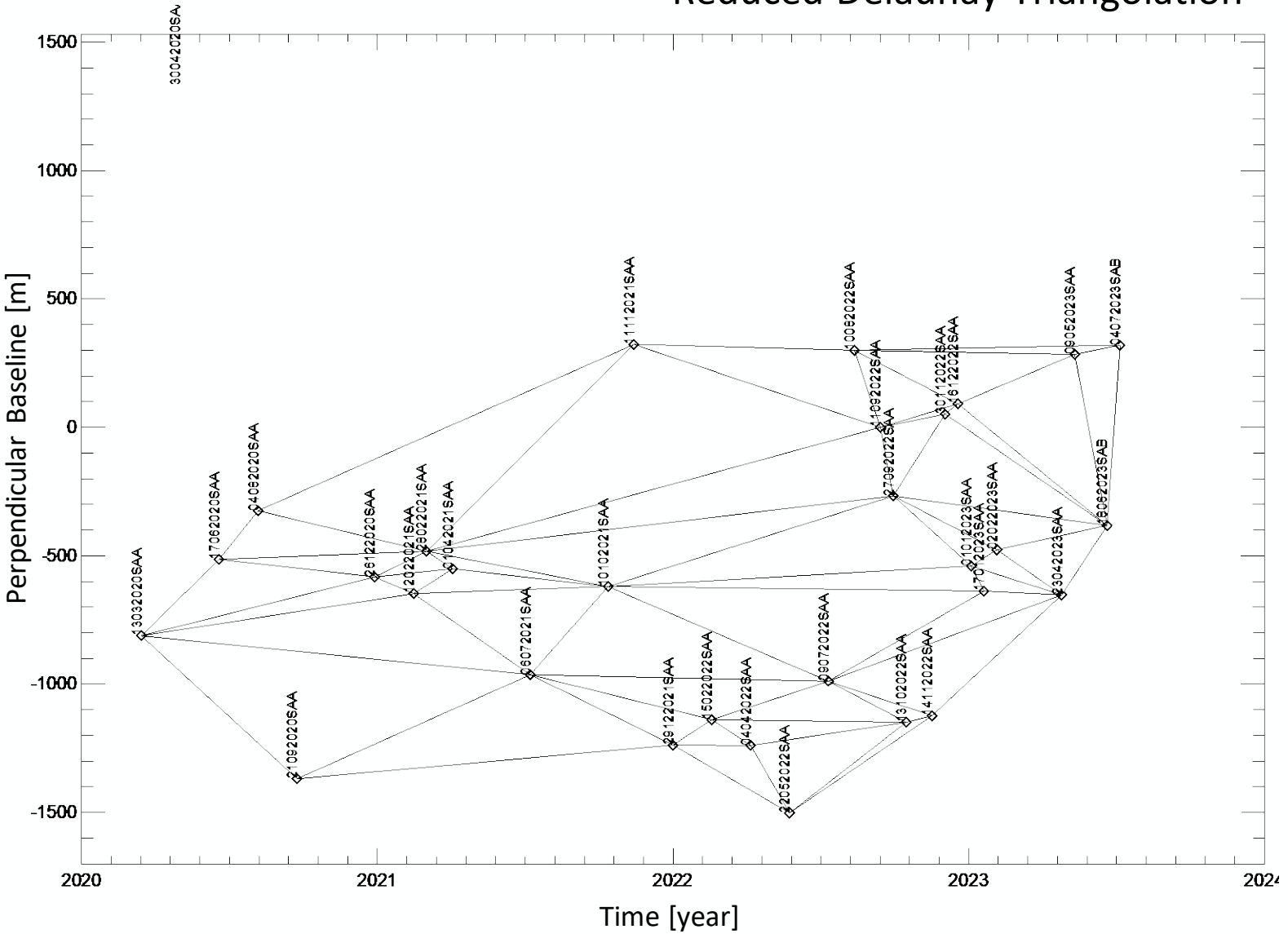

Stripmap P-SBAS processing chain for SAOCOM L1A data processing: PhU problem

Napoli Bay Area

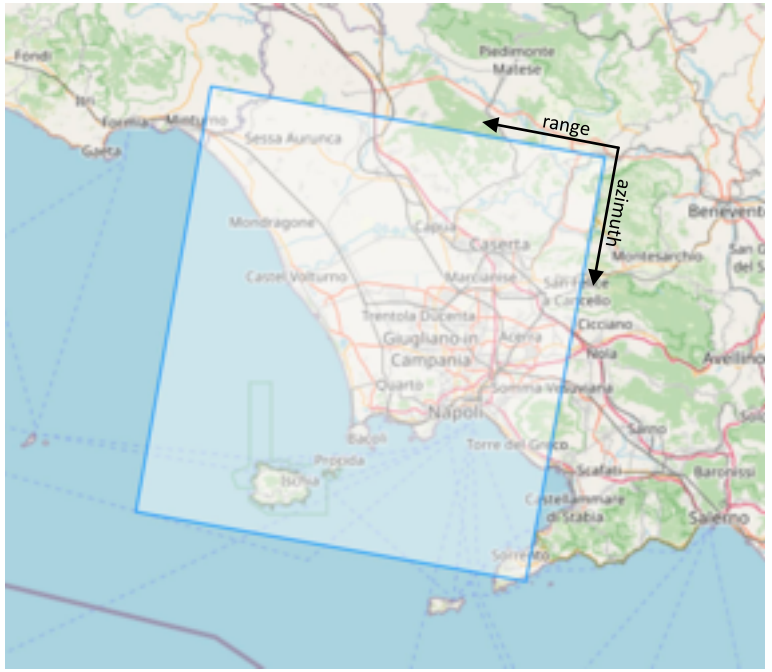

Baseline constraints

Temporal Baseline <= 600 days

Perpendicular Baseline <= 1500 m

Reduced Delaunay Triangolation

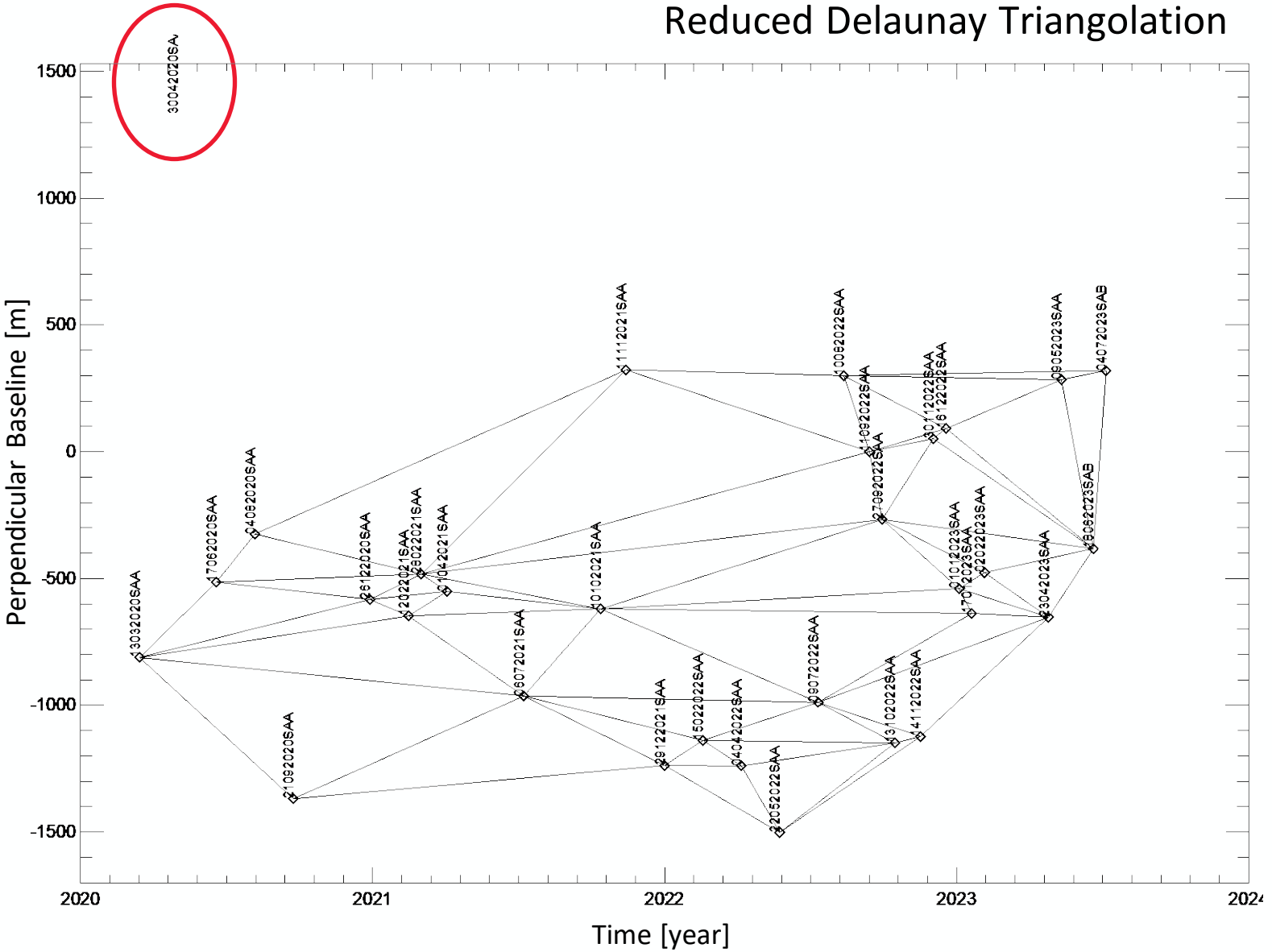

Stripmap P-SBAS processing chain for SAOCOM L1A data processing: PhU problem

Napoli Bay Area

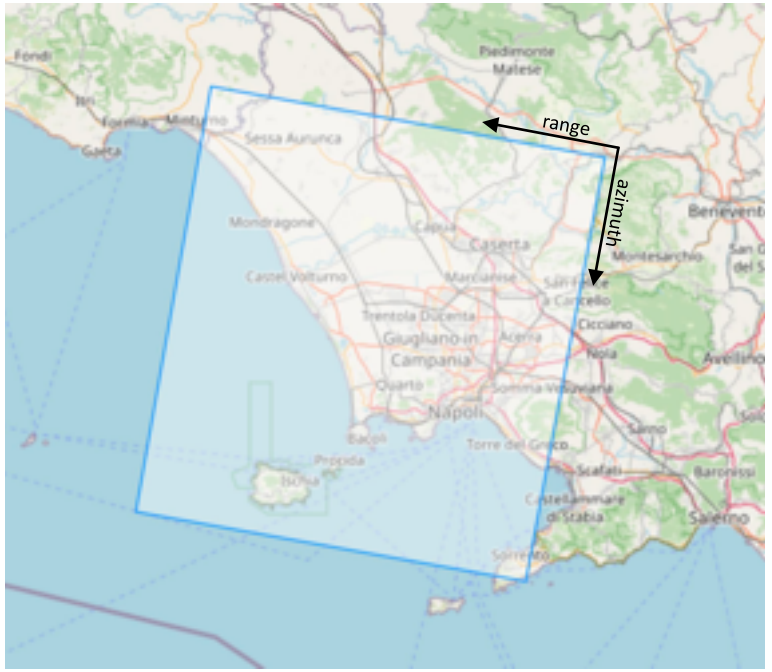

Baseline constraints

Temporal Baseline <= 600 days

Perpendicular Baseline <= 1500 m

Redundant Interferograms network

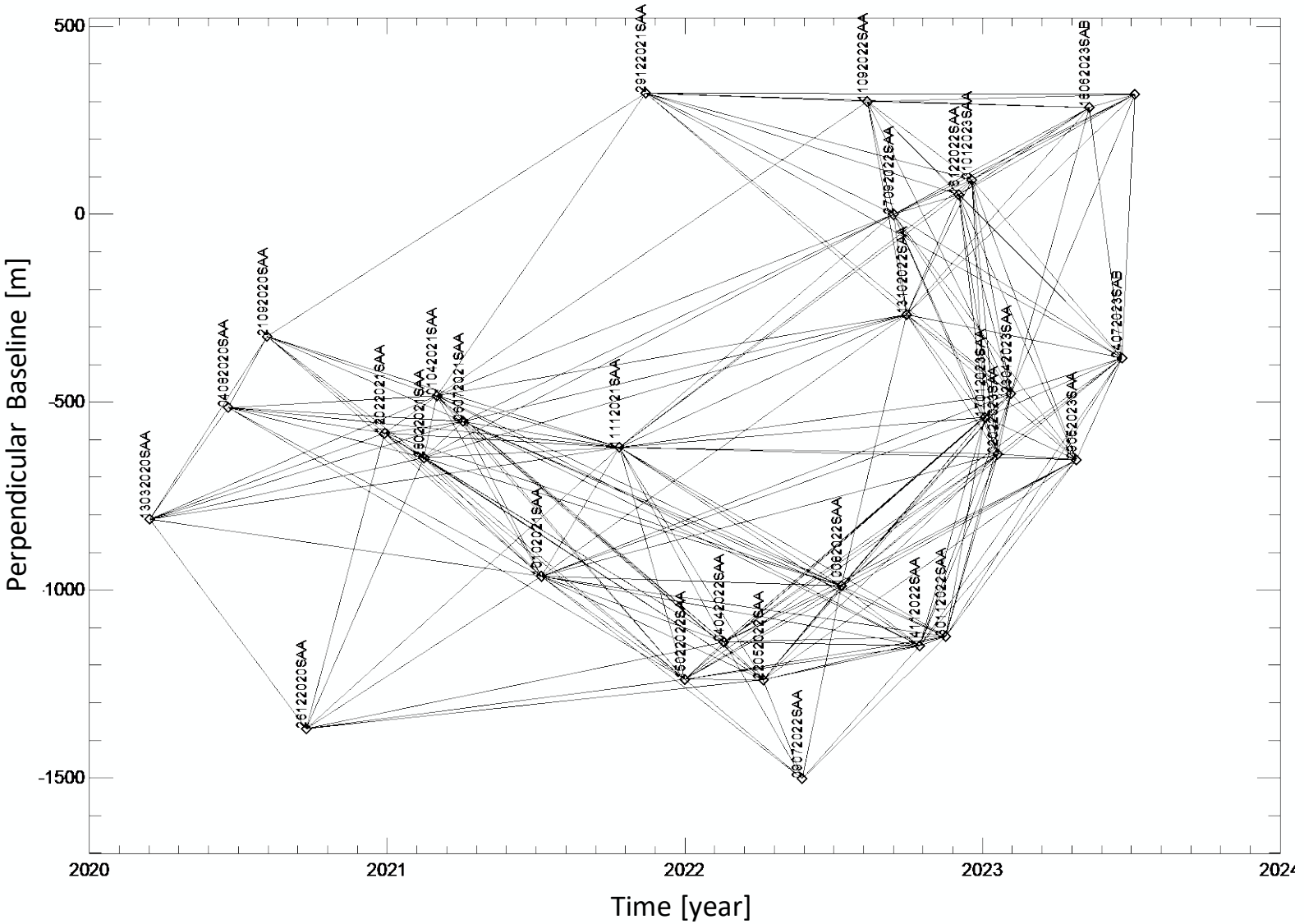

Displacement time-series generation over Campi Flegrai caldera

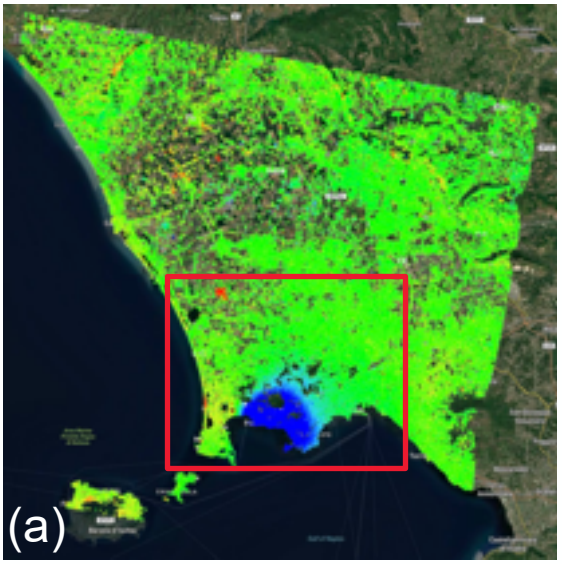

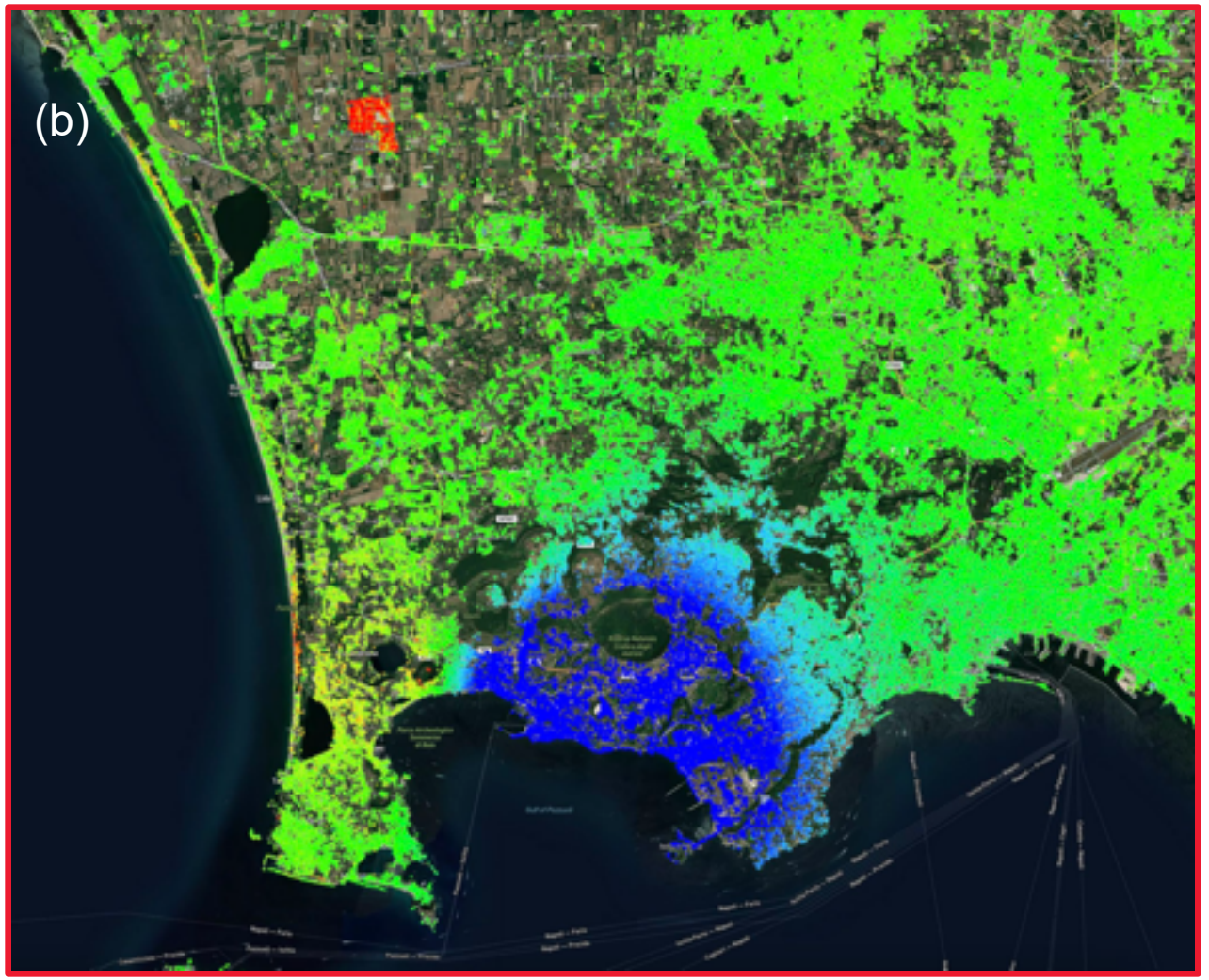

Mean LOS velocity
-2< >2
[cm/year]

Panel (a) shows a **mean deformation velocity** map obtain by processing the descending S4 SAOCOM L1A dataset over **CF caldera AoI**.

Panel (b) show a zoom over the **CF caldera**.

Displacement time-series generation over Campi Flegrai caldera

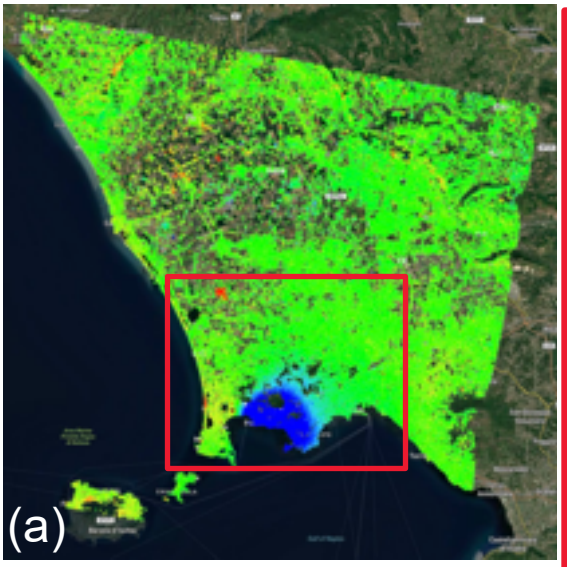

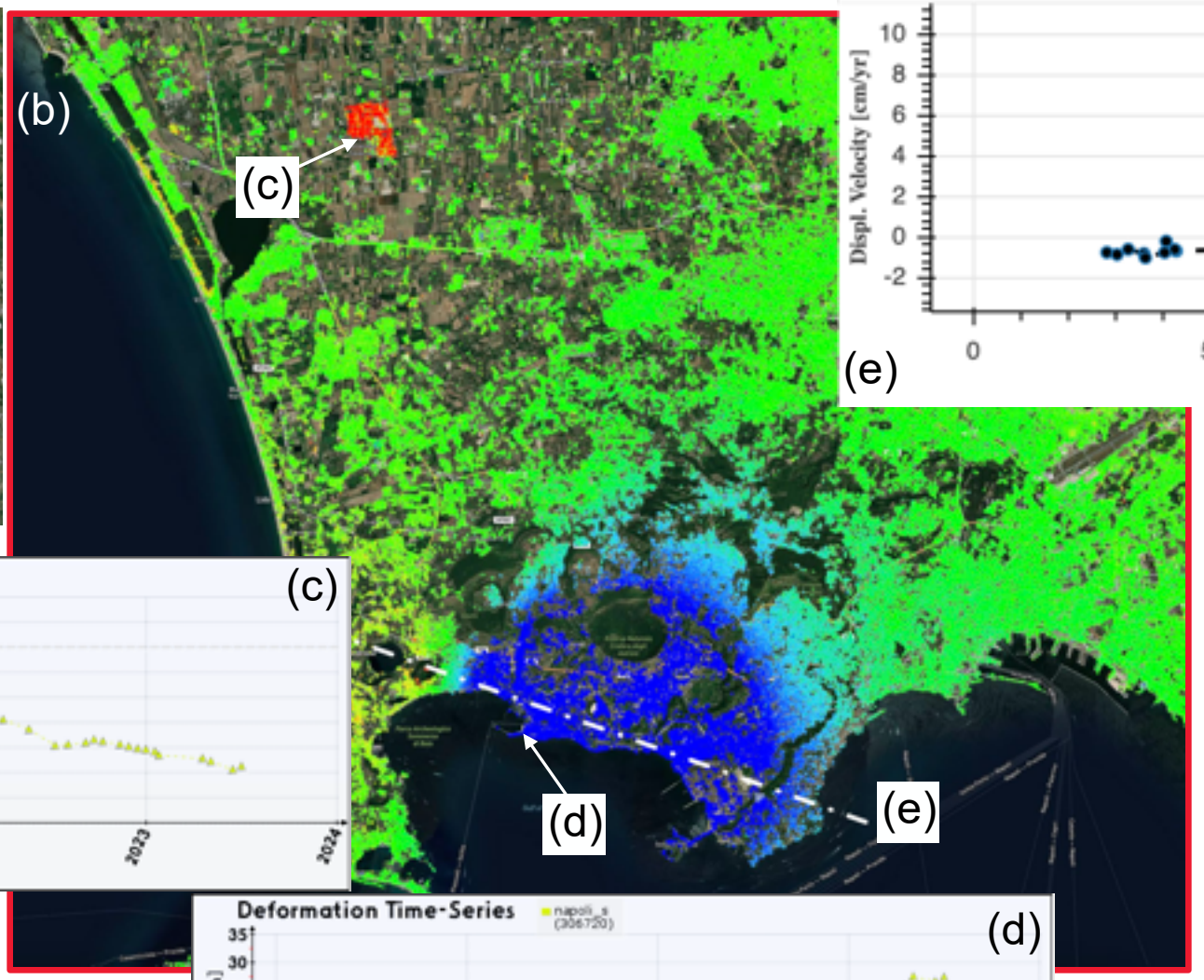

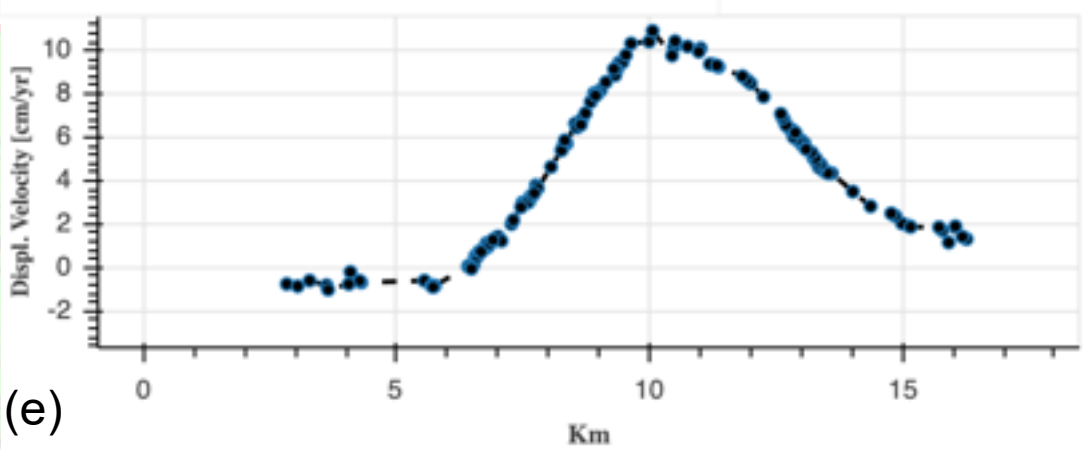

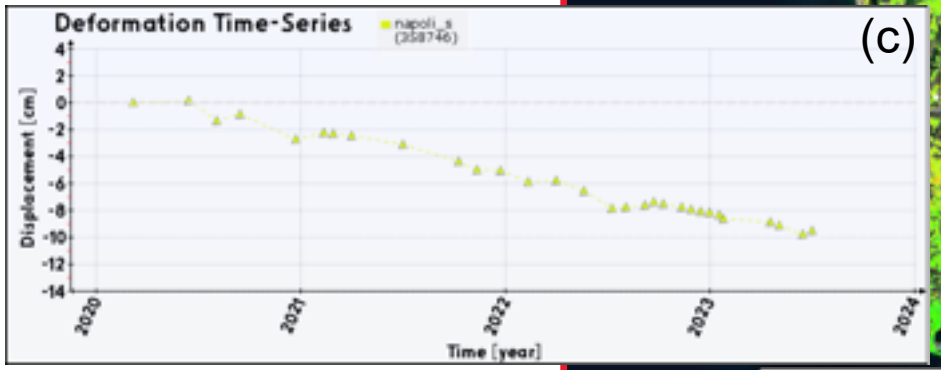

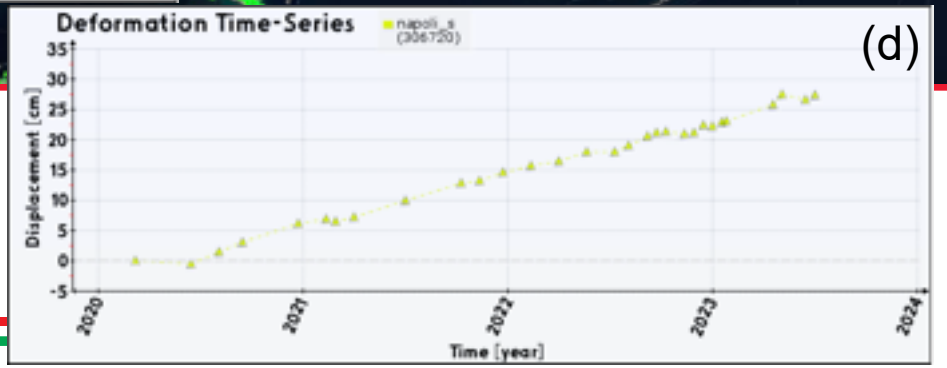

Panel (c) shows a plot of a pixel located in a **huge dump**.

Panel (d) reports a plot of the displacement time-series in a pixel located within the **Pozzuoli harbour**, which represents the area affected by the maximum of the displacement.

Panel (e) is a **profile of the mean deformation velocity** values that crosses the **CF caldera** and that shows the well-known radial geometry deformation pattern affecting the area.

Displacement time-series generation over Tuscany region

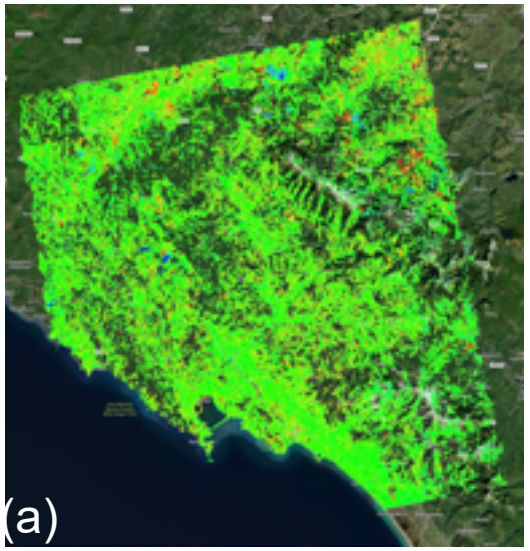

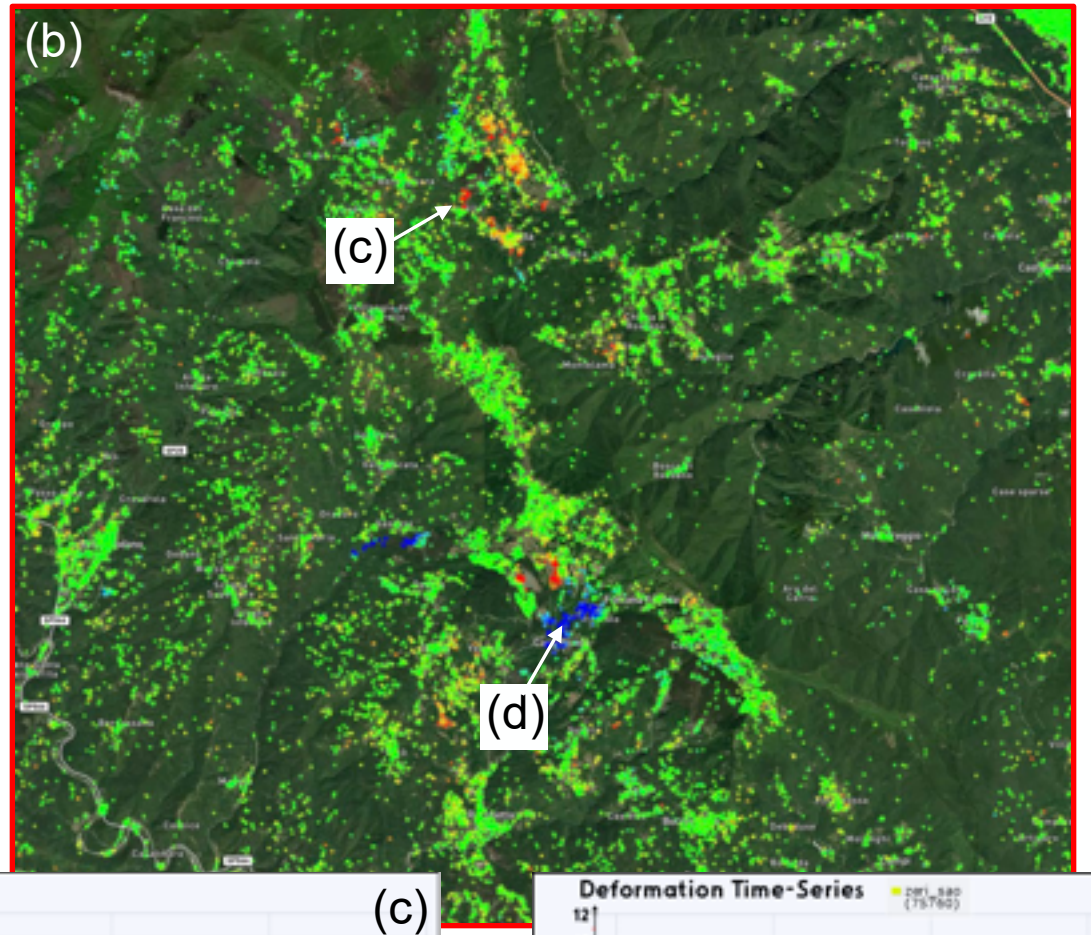

Mean LOS velocity
-2< >2
[cm/year]

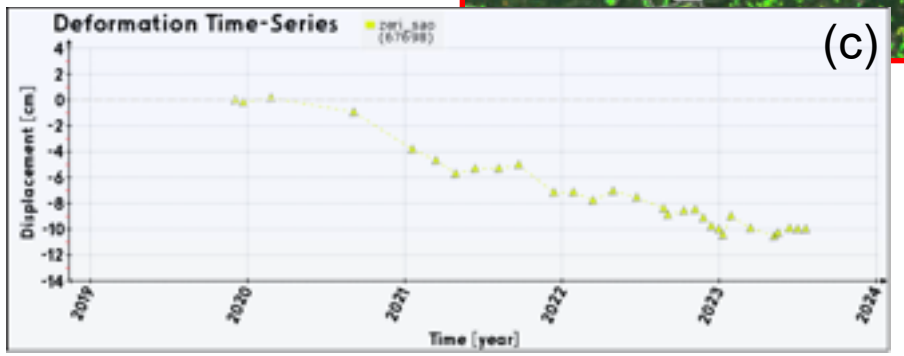

Panel (a) shows a **mean deformation velocity** map obtained by processing the ascending S3 SAOCOM L1A dataset over **Tuscany region**.

Panel (b) shows a zoom over the **Zeri AoI,** which is affected by several active landslides also in urban area.

Panels (c) and (d) report plots of the **displacement time-series** in two pixels located in correspondence of **Zeri** and **Fontana Fredda hamlets**.

Improvement, in terms of final measurements points number, that we can obtain through the P-SBAS analysis with SAOCOM-1 data (comparison between C and L band)

Improvement, in terms of final measurements points number, that we can obtain through the P-SBAS analysis with SAOCOM-1 data (comparison between C and L band)

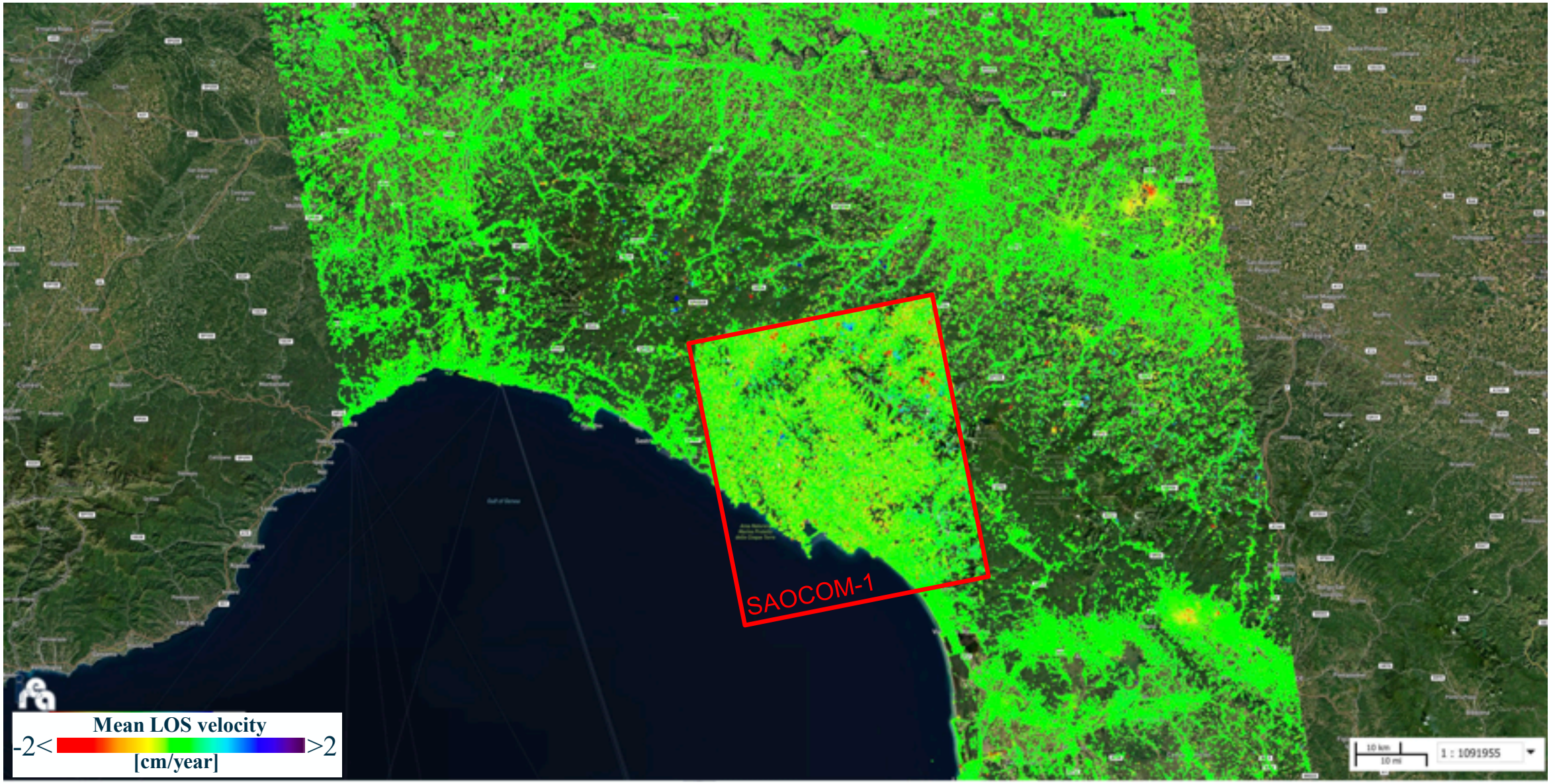

Improvement, in terms of final measurements points number, that we can obtain through the P-SBAS analysis with SAOCOM-1 data (comparison between C and L band)

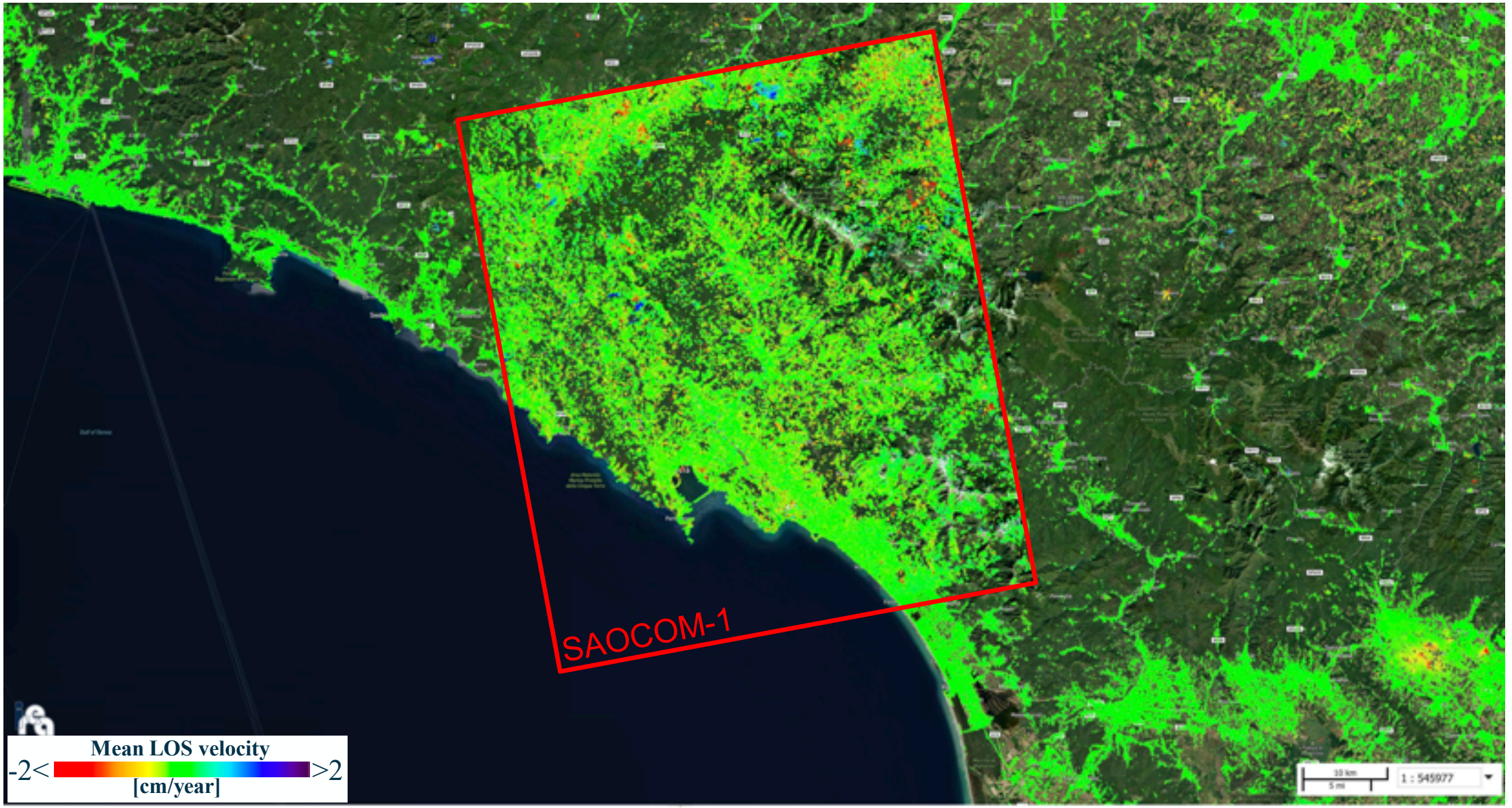

Improvement, in terms of final measurements points number, that we can obtain through the P-SBAS analysis with SAOCOM-1 data (comparison between C and L band)

Sentinel-1 P-SBAS analysis

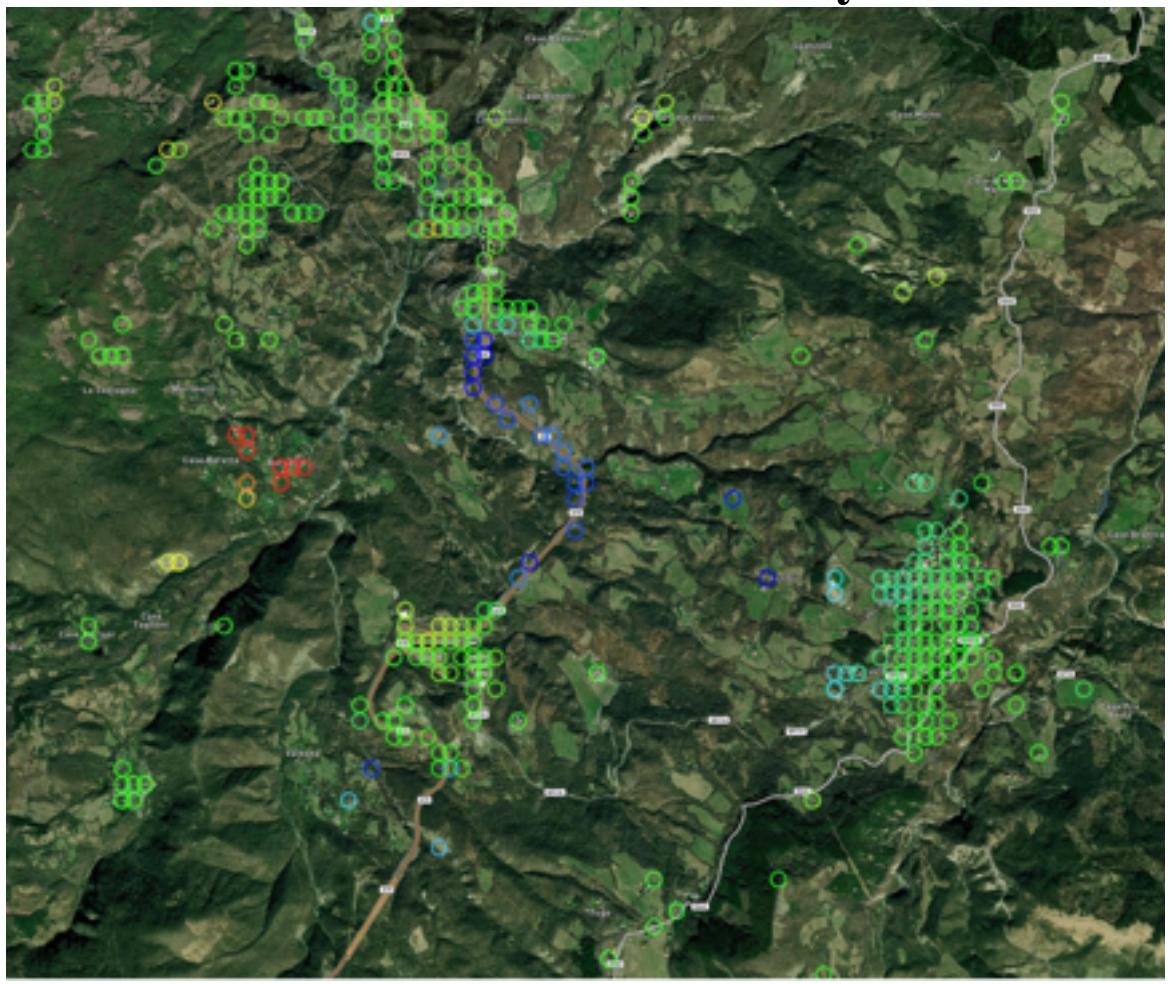

Mean LOS velocity
-2< >2
[cm/year]

SAOCOM-1 P-SBAS analysis

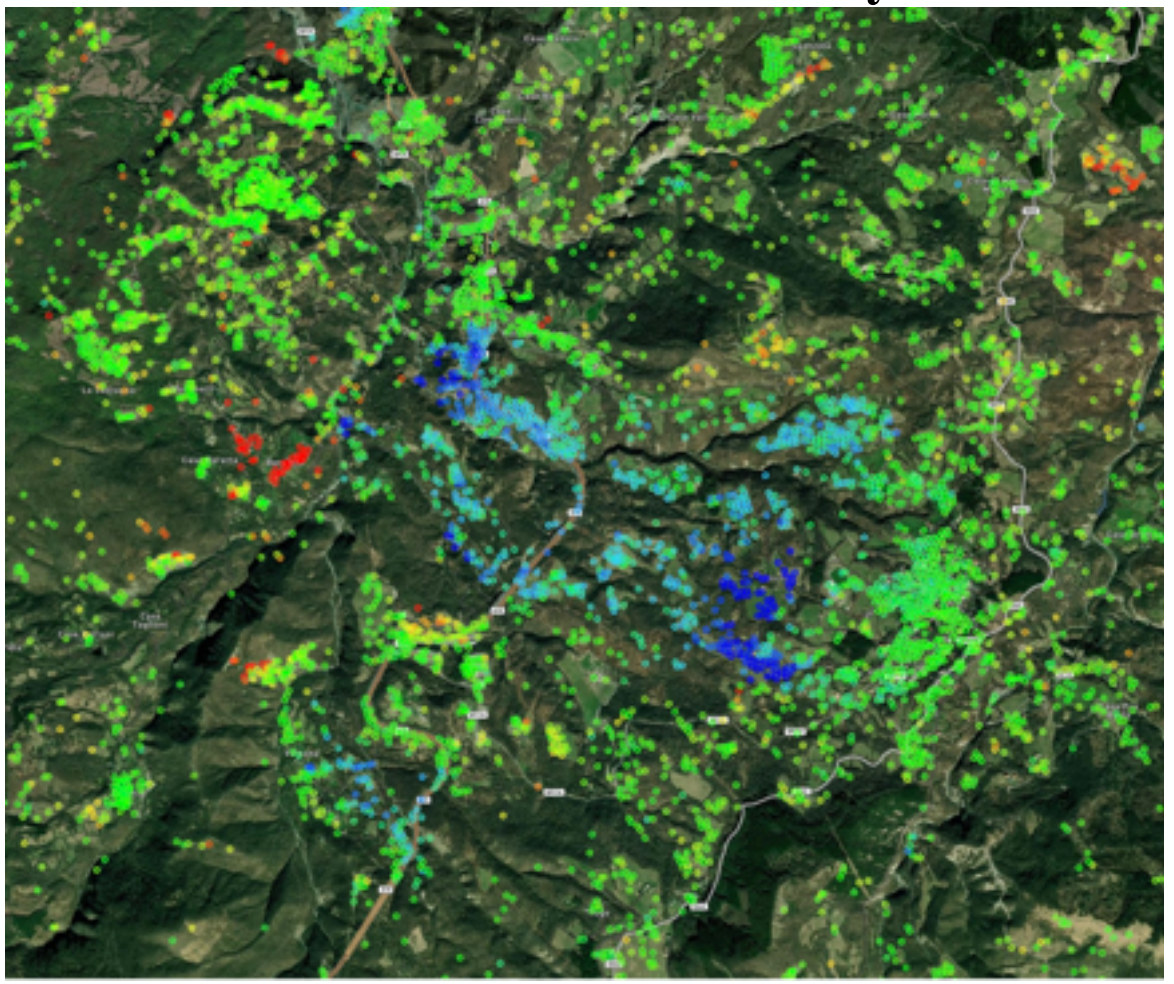

Mean LOS velocity
-2< >2
[cm/year]

Improvement, in terms of final measurements points number, that we can obtain through the P-SBAS analysis with SAOCOM-1 data (comparison between C and L band)

Sentinel-1 P-SBAS analysis

SAOCOM-1 P-SBAS analysis

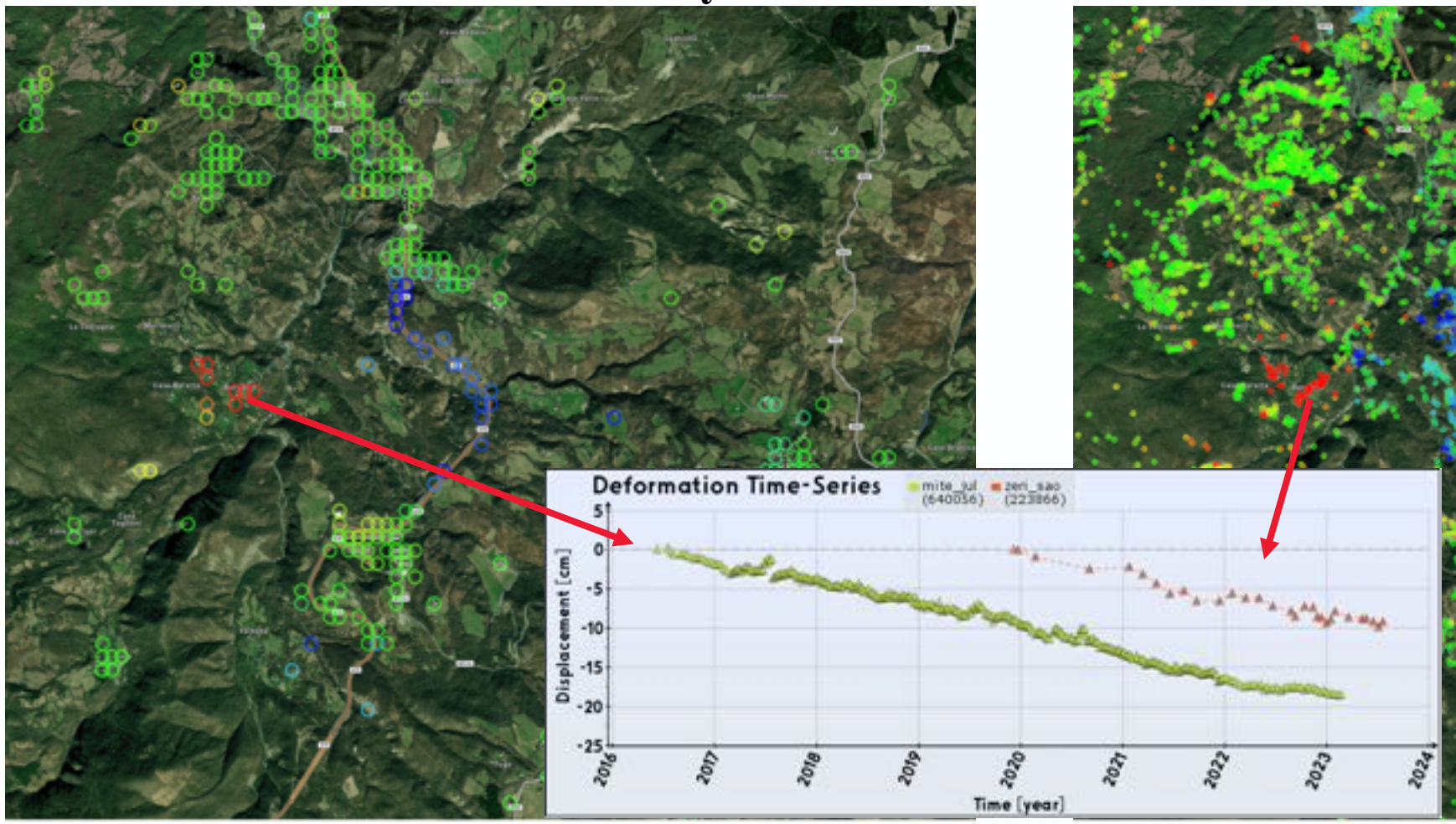

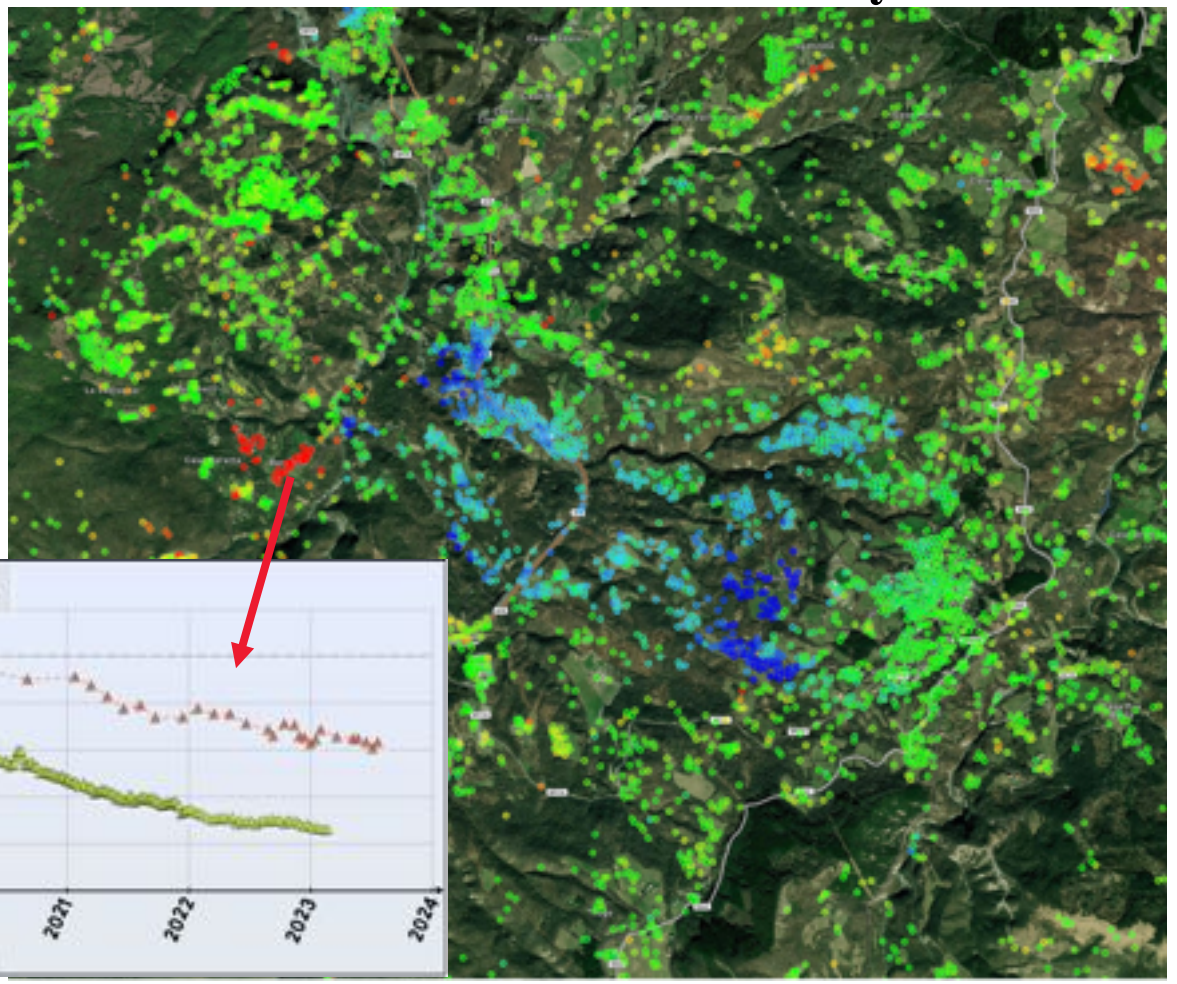

Mean LOS velocity
-2< >2
[cm/year]

Mean LOS velocity
-2< >2
[cm/year]

P-SBAS high resolution analysis over metallic infrastructures (Bridge of "Music" - Rome) (comparison between X and L band)

CSK-CSG 2011-2021 (λ ~ 3.1 cm)

LOS mean deformation CSK-CSG velocity

<- 1 > 1

[cm/year]

SAOCOM-1 2020-2023 (λ ~ 23.5 cm)

LOS mean deformation SAOCOM-1 velocity

<- 3 > 3

[cm/year]

P-SBAS high resolution analysis over metallic infrastructures (Bridge of "Music" - Rome) (comparison between X and L band)

CSK-CSG 2011-2021 (λ ~ 3.1 cm)

SAOCOM-1 2020-2023 (λ ~ 23.5 cm)

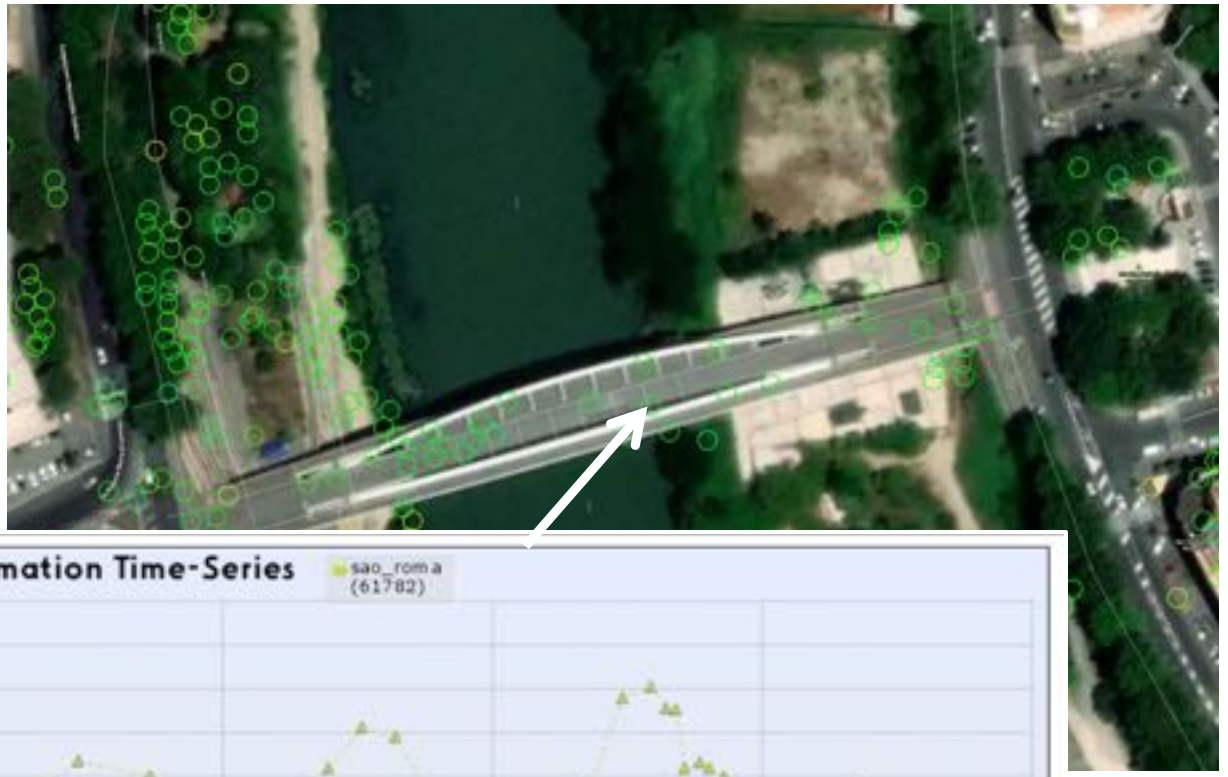

LOS mean deformation CSK-CSG velocity

<- 1 > 3

[cm/year]

Surface deformation retrieval of the February 2023 South-East Turkey and Northern Syria Mw 7.8 and Mw 7.5 seismic events through SAOCOM-1 co-seismic SAR image analysis

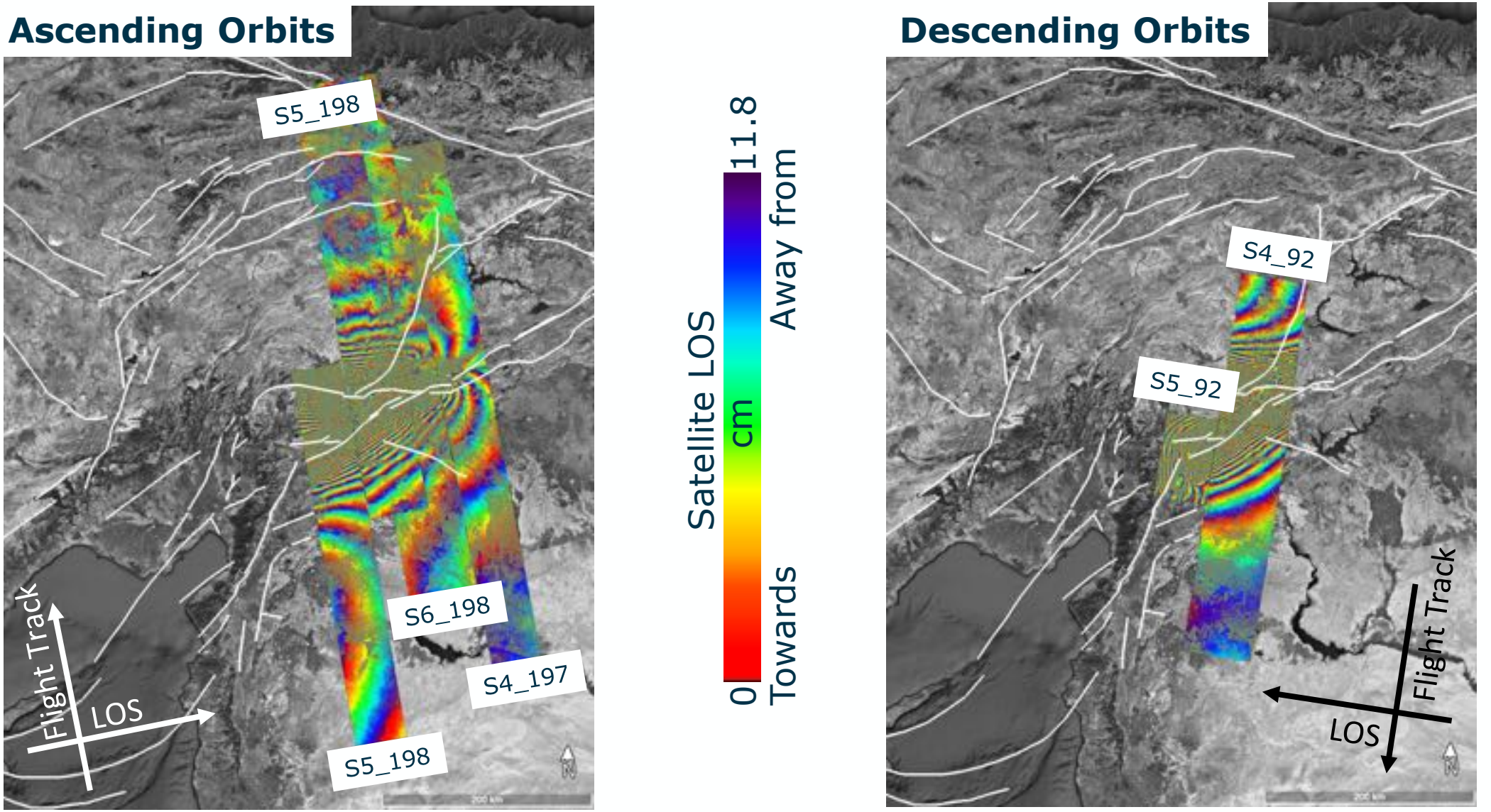

Azimuth Pixel-Offset

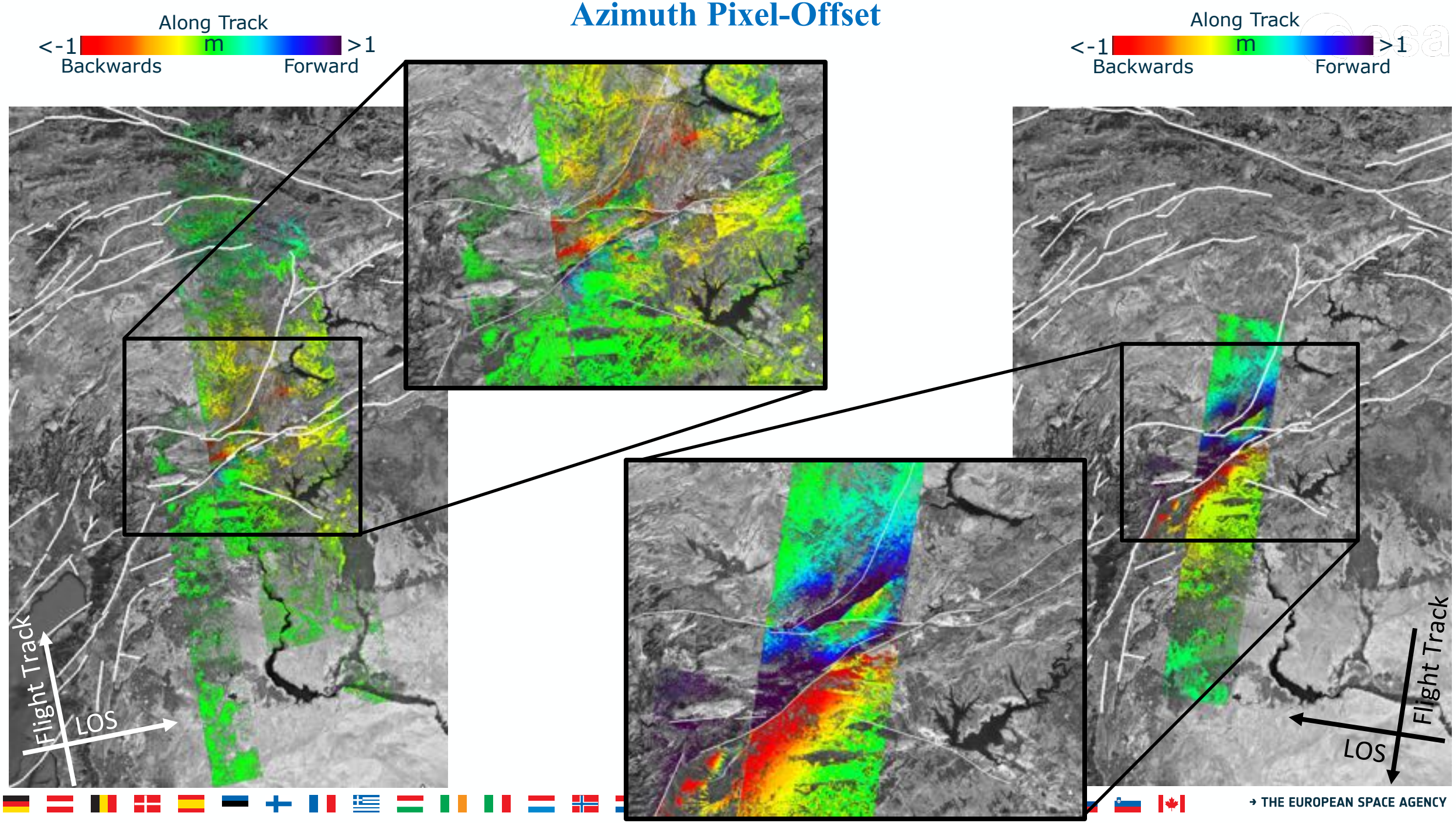

Slant Range Pixel-Offset

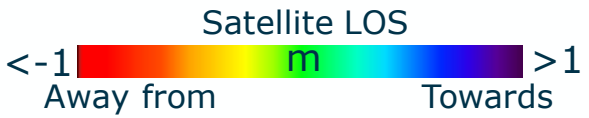

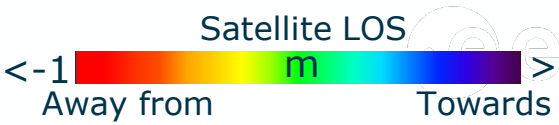

Ascending Orbits

Descending Orbits

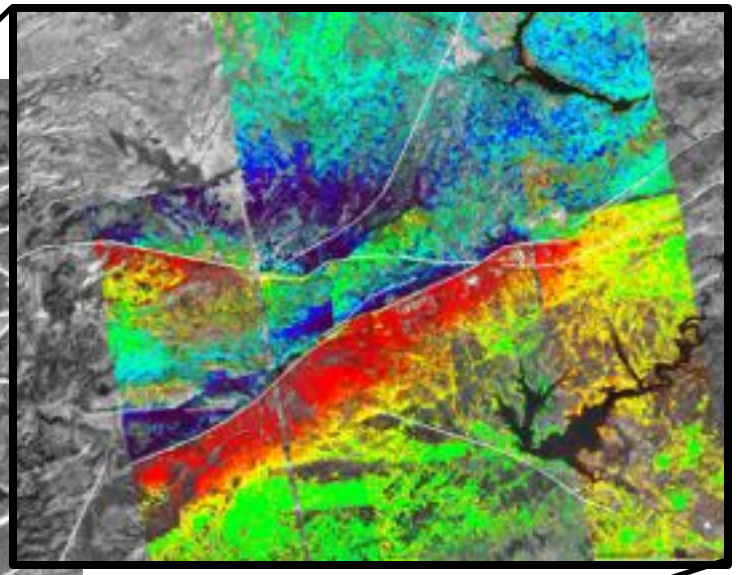

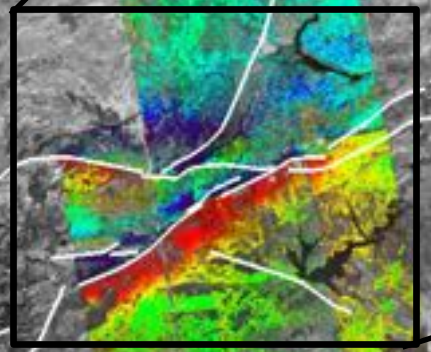

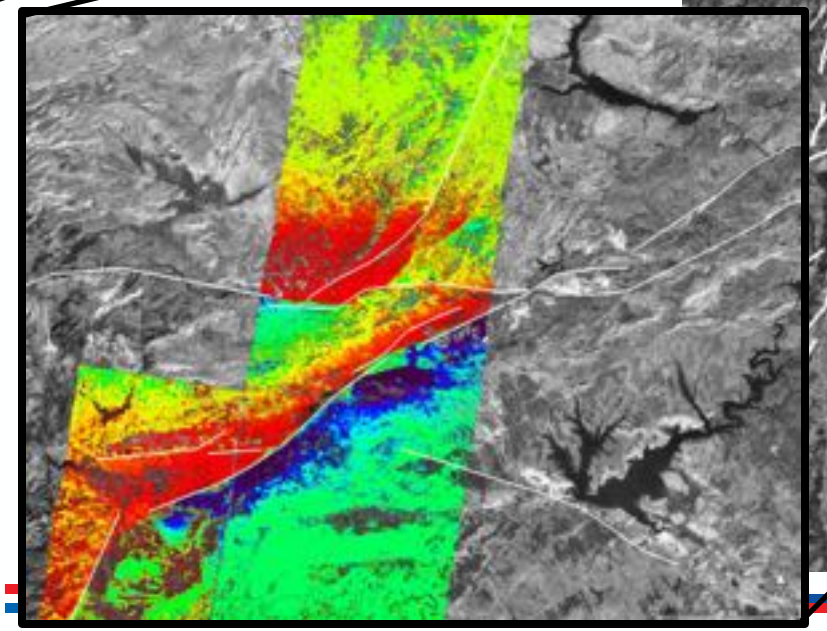

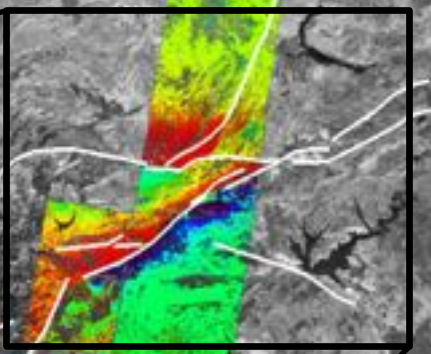

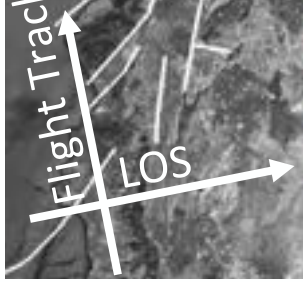

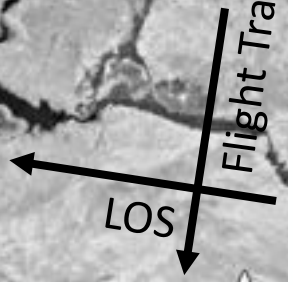

Reconstruction of the 3D deformation field

Vertical Component

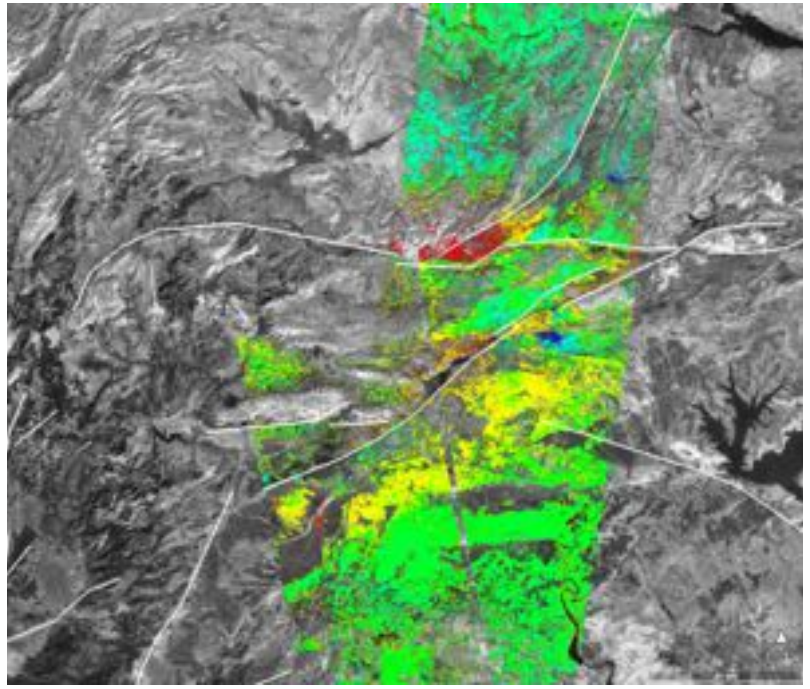

Down
<-1 m >1
Up

East Component

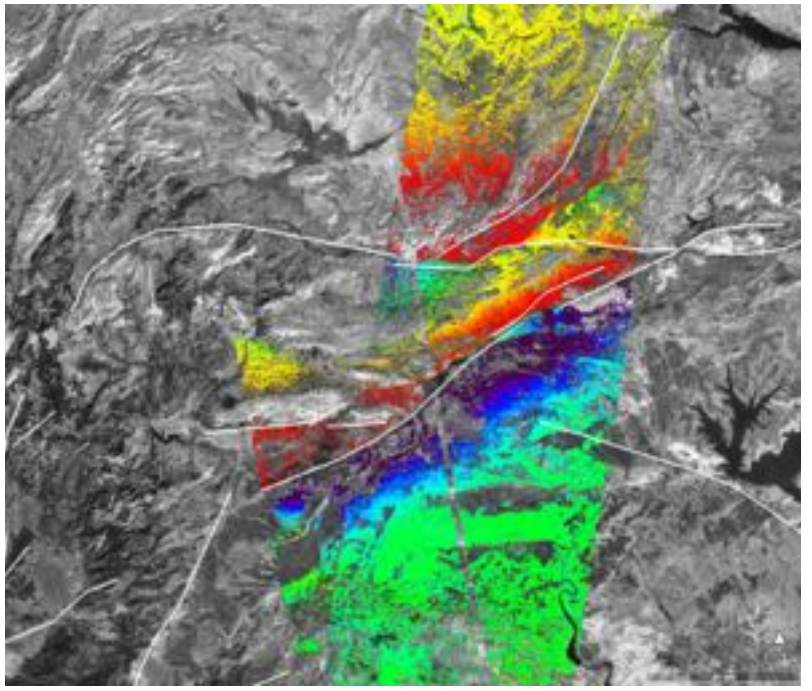

West
<-1.5 m >1.5
East

North Component

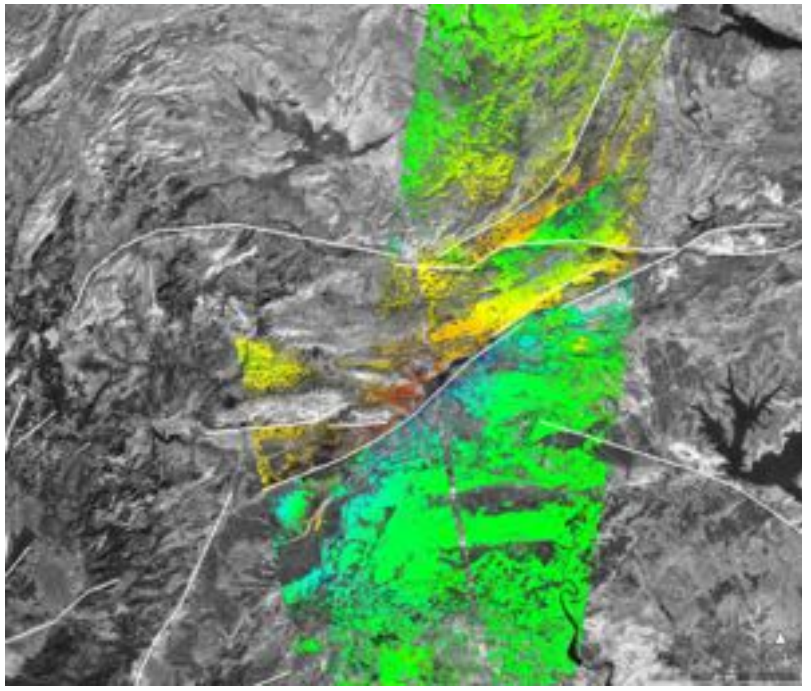

South
<-3 m >3
North

De Luca, C., Zinno, I., Manunta, M., Lanari, R., & Casu, F. (2017). Large areas surface deformation analysis through a cloud computing P-SBAS approach for massive processing of DInSAR time series. *Remote Sensing of Environment*, *202*, 3-17.

Focusing issues of the SLC SAOCOM data processed before the July 15, 2021 and state vectors inaccuracy

Campi Flegrei Ascending S4

No phase preserving behavior and residual phase ramps probably due to state vectors inaccuracy

Campi Flegrei Descending S4

Pair =23042020_01112020 - $\mathbf{B}_{perp}$ = 288m - $\mathbf{B}_{temp}$ = 192 days

Orbit = 23042020 (OLF) - 01112020 (OLVF)

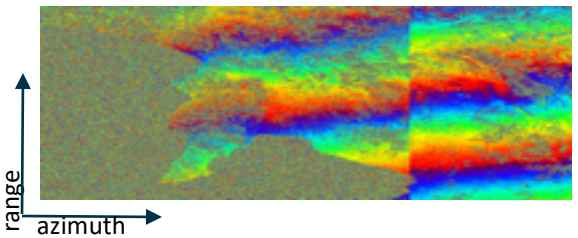

Pair =13032020_26122020 - $\mathbf{B}_{perp}$ = 242m - $\mathbf{B}_{temp}$ = 288 days

Orbit = 13032020 (OLF) - 26122020 (OLVF)

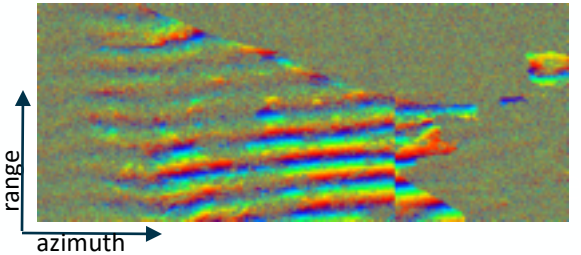

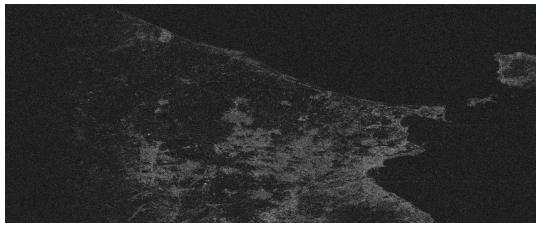

Focusing issues of the SLC SAOCOM data processed before the July 15, 2021 and state vectors inaccuracy

Campi Flegrei Ascending S4

No phase preserving behavior and residual phase ramps probably due to state vectors inaccuracy

Campi Flegrei Descending S4

Pair =23042020_01112020 - $\mathbf{B_{perp}}$ = 288m - $\mathbf{B_{temp}}$ = 192 days

Orbit = 23042020 (OLF) - 01112020 (OLVF)

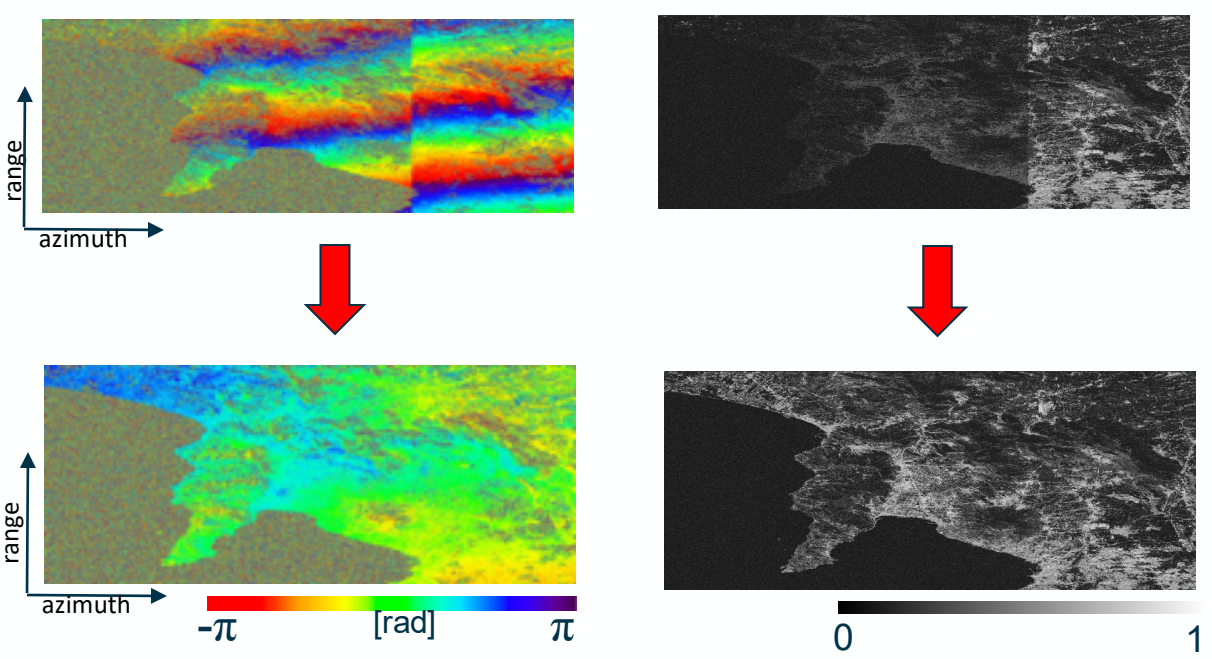

Pair =13032020_26122020 - $\mathbf{B_{perp}}$ = 242m - $\mathbf{B_{temp}}$ = 288 days

Orbit = 13032020 (OLF) - 26122020 (OLVF)

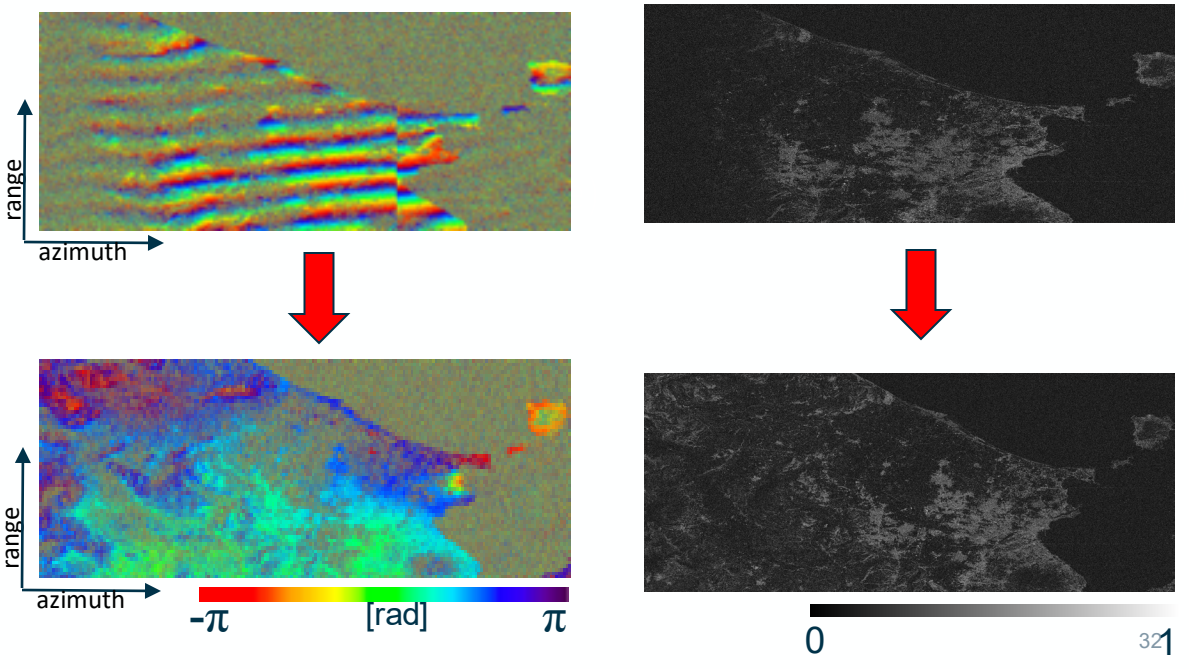

Suspected Ionospheric issues on the SLC SAOCOM data: Litli-Hrútur eruption-Iceland

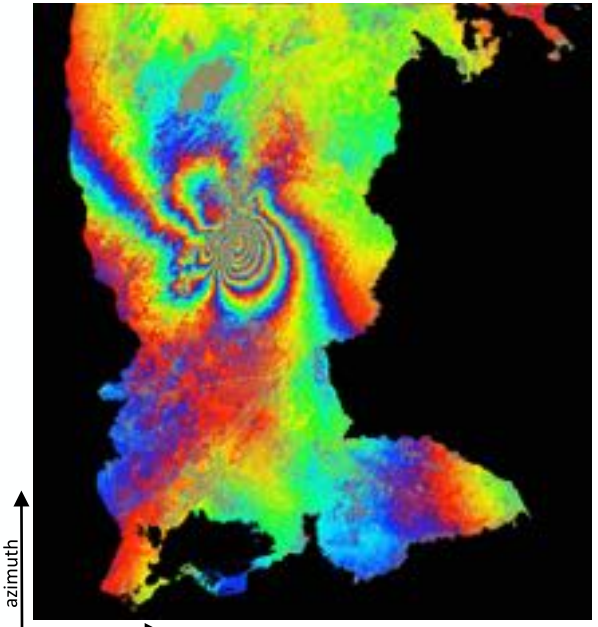

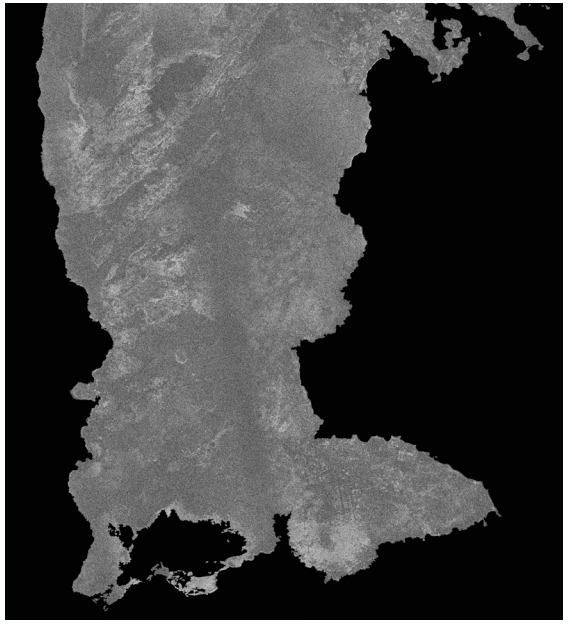

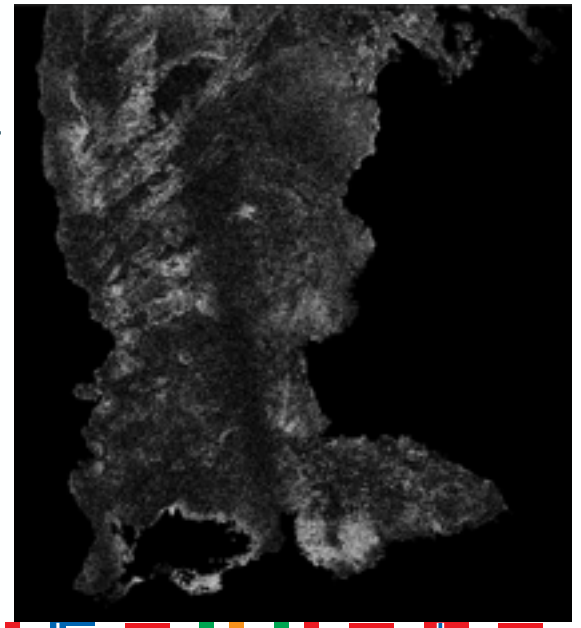

SAOCOM-L1A - ASC - S6

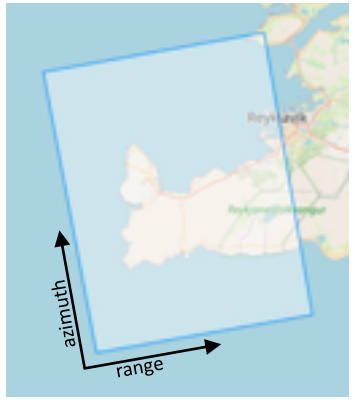

Pixel-Offset Displacement Analysis

Slant Range

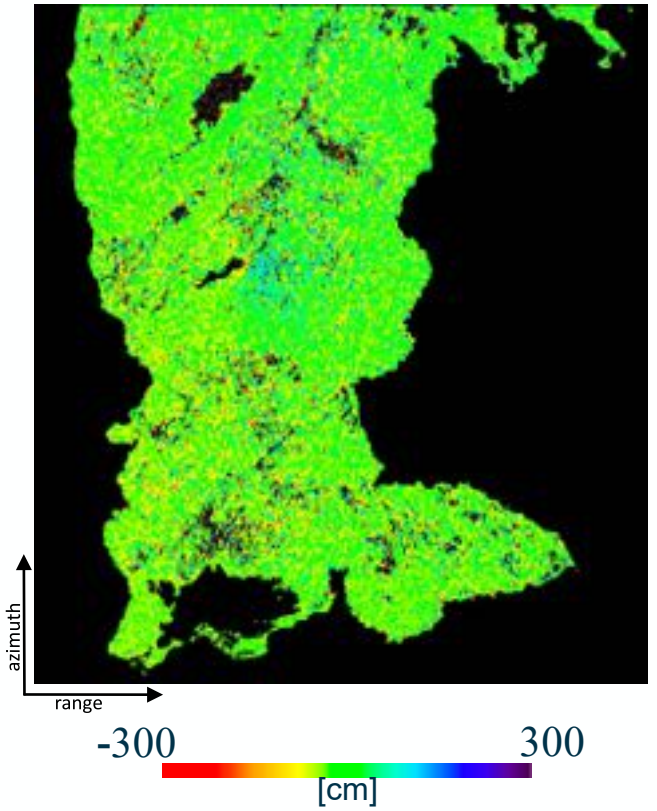

Azimuth

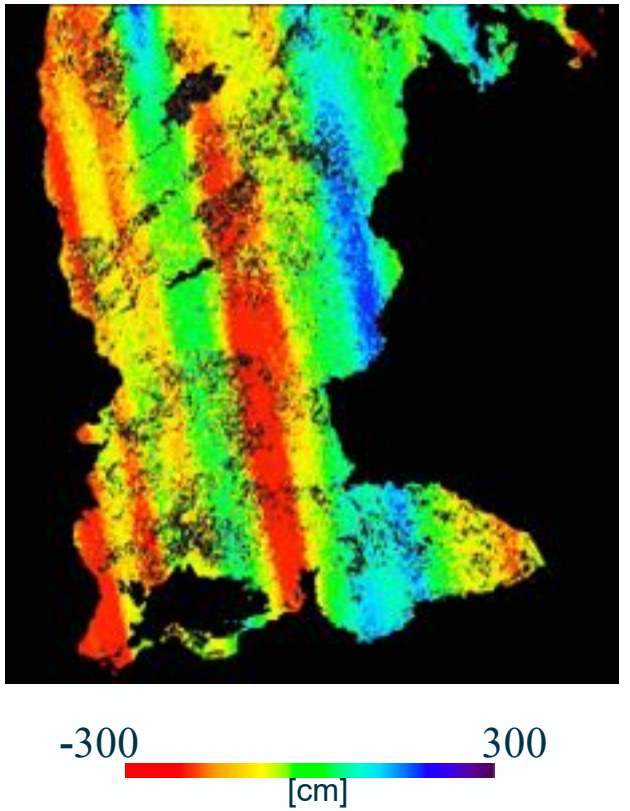

Thank you for your attention !

deluca.c@irea.cnr.it

Displacement time-series generation over Sicily region/Mount Etna volcano

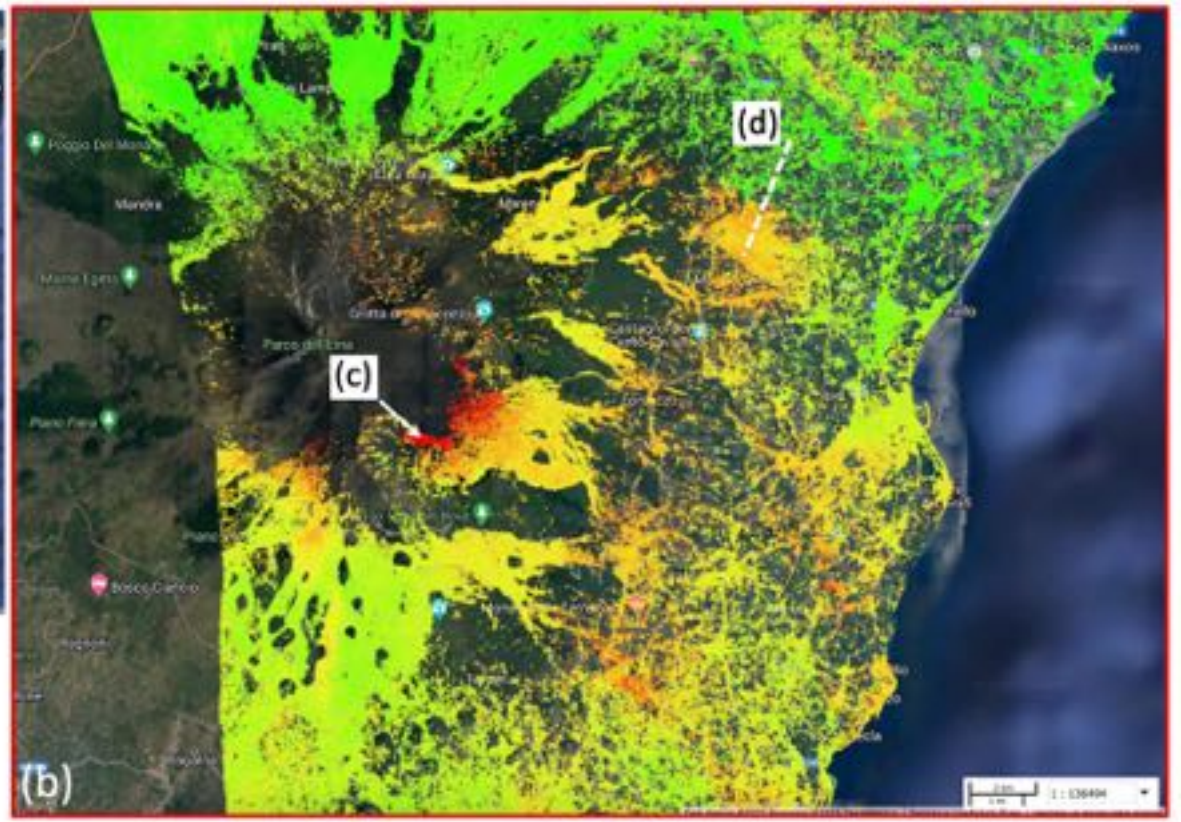

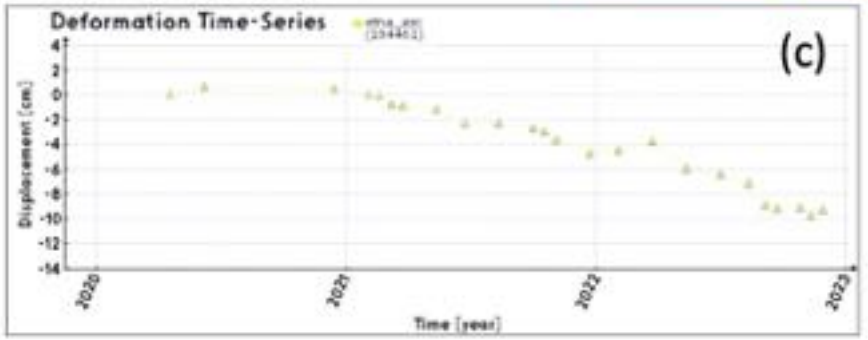

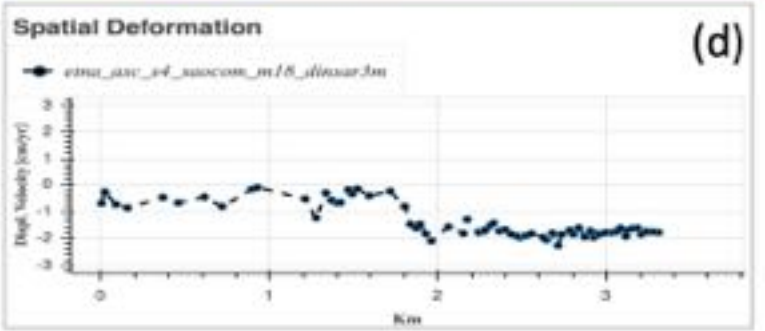

Panel (a) shows a **mean deformation velocity** map obtain by processing the ascending S4 SAOCOM L1A dataset over **Sicily region**.

Panel (b) shows a zoom over **Mount Etna volcano**.

Panel (c), instead, reports a plot of the displacement time-series in a pixel located within the **Valle del Bove**, which represents the area affected by strong subsidence phenomena.

Panel (d) is a **profile of the mean deformation velocity** values that crosses the **Pernicana fault** that highlights a well-known differential displacement between north and south edges of the fault .

SAOCOM-1 DInSAR and Pixel Offset measurements

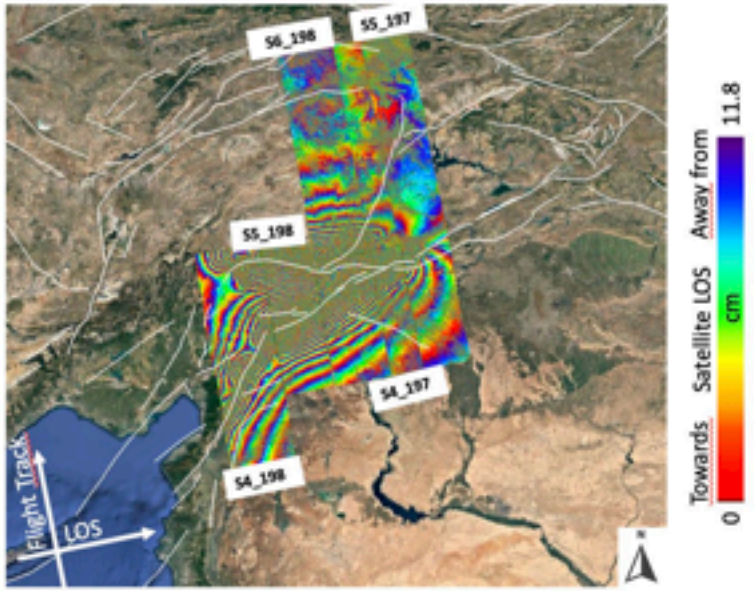

TRACK	Interferometric pairs
S4_197	02.05.2022SAB_14.02.2023SAB
S4_197	21.07.2022SAB_14.02.2023SAB
S4_198	27.04.2022SAB_22.04.2023SAA
S5_197	11.02.2022SAB_02.03.2023SAB
S5_197	27.02.2022SAB_02.03.2023SAB
S5_198	29.05.2022SAB_30.04.2023SAA
S6_198	14.06.2022SAB_25.02.2023SAB
S6_198	30.06.2022SAB_25.02.2023SAB

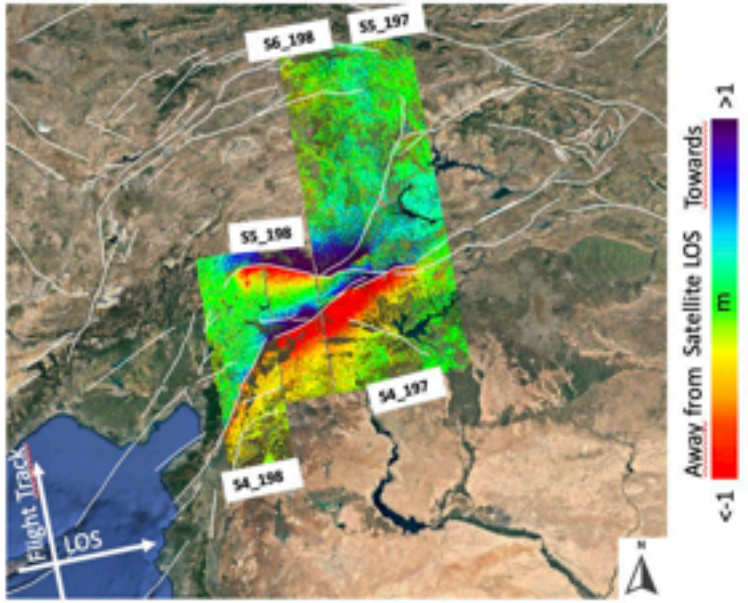

Range Pixel Offset

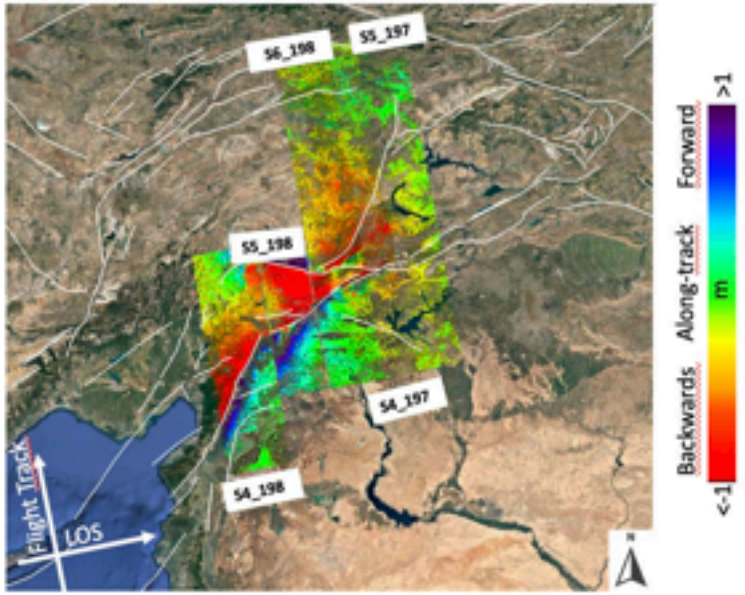

Azimuth Pixel Offset